



Evaluation of MODIS Collection 6 aerosol retrieval algorithms over Indo-Gangetic Plain: Implications of aerosols types and mass loading[☆]

Alaa Mhawish^a, Tirthankar Banerjee^{a,b,*}, David M. Broday^c, Amit Misra^d, Sachchida N. Tripathi^d

^a Institute of Environment and Sustainable Development, Banaras Hindu University, Varanasi, India

^b DST-Mahamana Centre of Excellence in Climate Change Research, Banaras Hindu University, Varanasi, India

^c Civil and Environmental Engineering, Technion, Haifa, Israel

^d Department of Civil Engineering, Indian Institute of Technology Kanpur, Kanpur, India

ARTICLE INFO

Keywords:

AERONET

AOD

Fine particulates

MODIS

Spatiotemporal comparison

IGP

Validation

ABSTRACT

This study evaluates the performance of MODerate resolution Imaging Spectroradiometer (MODIS) Collection 6 (C6) AOD retrieval algorithms, including Dark Target (DT) aerosol optical depth (AOD) at 3 and 10 km spatial resolutions, Deep Blue (DB) AOD at 10 km, and the merged DT-DB AOD at 10 km across the Indo-Gangetic Plain (IGP), South Asia. A total of 14,736 collocated Aqua MODIS C6 AOD at 550 nm were evaluated against AOD from six AERONET stations over IGP, measured during the satellite overpass (± 1 h) from 2006 to 2015. The effects of aerosol heterogeneity, in terms of both aerosol loading and the aerosol type, on the uncertainty of the satellite-borne AOD retrieval were examined. The DT algorithm at both resolutions (3 km and 10 km) overestimated the AOD by 14–25%, with only 51.37–61.29% of the retrievals falling within the expected error (EE). The DT 3 km algorithm underestimates the surface reflectance in comparison to the DT 10 km, with the latter outperforming the former both in terms of number of collocations and retrieval accuracy, especially over urban areas. The DB 10 km was able to retrieve AOD over both arid/desert regions and vegetated surfaces even under low aerosol loading conditions. Yet, its performance was still poor, with retrieval accuracy of 53.76%, low RMSE (0.214), and generally underestimated AOD across the IGP. The merged DT-DB AOD product was mostly dominated by DT retrievals (73%–100%), except over bright land surfaces and 56.03% of the merged DT-DB retrievals fell within the EE. The retrieval accuracy of MODIS C6 products was found to be strongly dependent on the estimated surface reflectance and the aerosol type. Across IGP, DB predicted the surface reflectance better while DT at both resolutions overestimated the surface reflectance at varying extent. For high aerosol loading conditions with varying aerosol size, retrieval accuracy of DT 10 km poses lower sensitivity while DT at 3 km exhibits larger uncertainty in estimating surface reflectance. In contrast, DB 10 km shows greater bias that depends on the aerosol size. For very high aerosol loading conditions, dominated by fine or mixed aerosols, all the algorithms have errors in the aerosol model. The DT 10 km, DB 10 km and the merged AOD performed almost equally within the threshold level while the DT 3 km showed the poorest performance in terms of retrieval accuracy and RMSE. We conclude that across IGP, DB 10 km AOD has the highest accuracy in retrieving fine mode aerosols while DT 10 km AOD has almost identical accuracy in retrieving varying aerosol types. For coarse dominated aerosols, when the dissimilarity between DT and DB remains highest, the merged AOD is found to have higher accuracy in retrieving AOD across IGP.

1. Introduction

Aerosol is an important component of the earth's climatic system which contributes to the single largest uncertainty in Earth's radiation budget (Boucher et al., 2013; Kumar et al., 2017a; Tripathi et al., 2007). These multi-component substances evolve either through natural processes (like biogenic and volcanic emissions) or by anthropogenic

activities (like combustion of fossil fuel, industrial processes, and biomass burning) before being disperse horizontally and vertically by atmospheric circulation (Singh et al., 2017a; Banerjee et al., 2015). Numerous studies have provided evidences of aerosols' influences on lateral transfer of radiant energy within the atmosphere (Boucher et al., 2013), radiative effects due to aerosol–radiation interactions (Ramana et al., 2010; Chen et al., 2010), modifications of cloud microphysical

[☆] Capsule: This study compares the Aqua MODIS C6 algorithms across IGP and assesses the quality of the products under varying aerosol loading and aerosol type conditions.

* Corresponding author at: Institute of Environment and Sustainable Development, Banaras Hindu University, Varanasi 221005, India.

E-mail address: tb.iesd@bhu.ac.in (T. Banerjee).

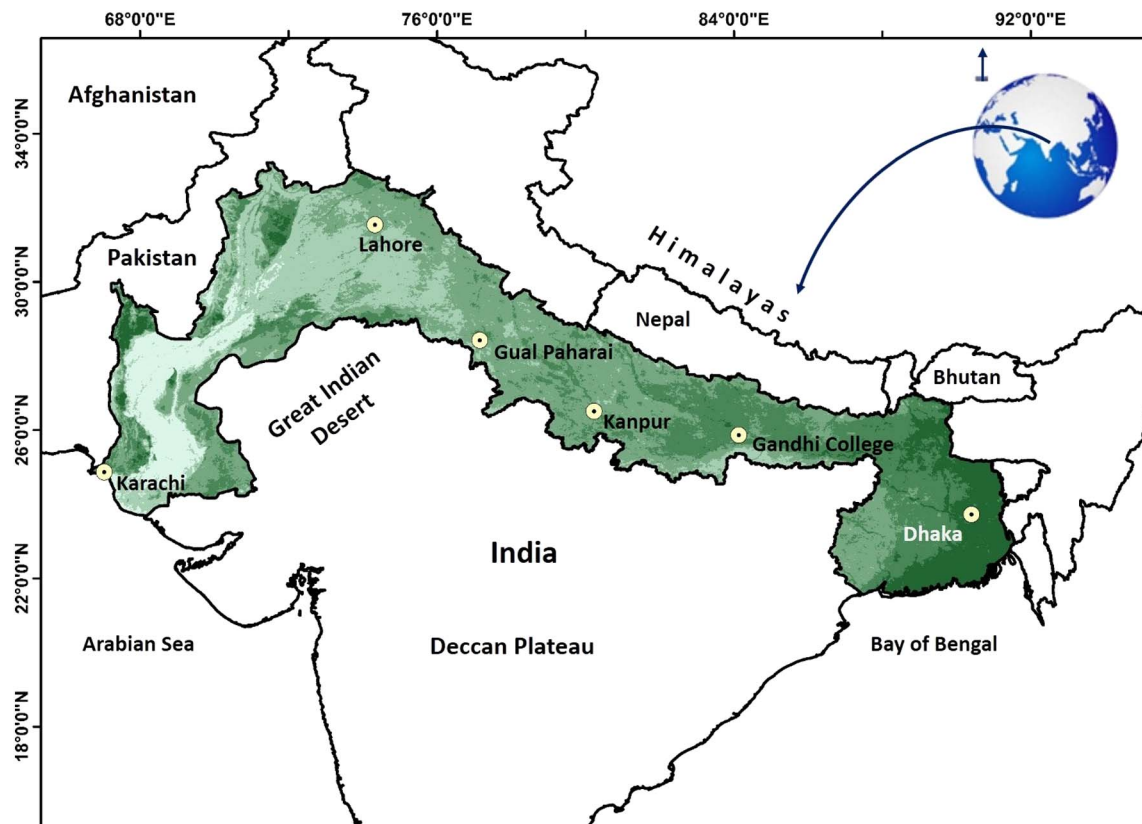


Fig. 1. Study area of the entire Indo-Gangetic Plain and the location of AERONET stations.

Note: The background image of IGP is the 2015 surface reflectance at $0.55 \mu\text{m}$ from MODIS (MOD09). The dark shade shows higher vegetated area while light shade depicts brighter surface.

properties (Seinfeld et al., 2016) and thereby influencing hydrological cycle (Ramanathan et al., 2001; Creamean et al., 2013), affecting regional food security (Burney and Ramanathan, 2014; Gupta et al., 2017) and ultimately deteriorating human health (Apte et al., 2015; Kumar et al., 2015a; WHO, 2014; Banerjee et al., 2017a, 2017b). The emissions, micro-physical properties, mixing-states of aerosols and its precursors provide unique evidences of its impacts on climate change. However, precise quantification of the aerosols feedback on climate still pose considerable uncertainties due to inconsistency across studies (Boucher et al., 2013) and high spatio-temporal variations in physio-chemical characteristics of aerosols (Kumar et al., 2017b; Sen et al., 2017; Banerjee et al., 2015). Although, ground-based measurement recognizes the optical and microphysical properties of aerosols, satellite based retrievals mostly complement this information by providing systematic retrieval on both local and global scales (Kaufman et al., 2005; Kahn et al., 2010) and by constraining aerosol parameterization in atmospheric models. Due to availability of diversified datasets, applications of satellite retrieved information has been exploited in numerous researches for estimating ground-level particulate concentration (Sorek-Hamer et al., 2013a), exposure and mortality studies (Van Donkelaar et al., 2010; Apte et al., 2015), crop yield/health simulation (Fang et al., 2011), recognizing pollution episodes (Kumar et al., 2016, 2017a) and forecasting of climate extremes (Sorek-Hamer et al., 2013b; Dey et al., 2004). However, satellite based information includes some fundamental errors due to instrumentation and retrieval algorithms which necessitate extensive validation against ground-based measurements (Li et al., 2014a, 2014b). Possible validation of satellite products will therefore help in reducing various uncertainties for recognizing aerosol ground-level concentrations, and for simulating aerosol-climate interactions and to forecast air quality at both the local and regional scales.

Among various sensors that routinely provide aerosols columnar

properties throughout the globe, Moderate Resolution Imaging Spectrometer (MODIS) on board the Terra and Aqua satellites are recognized as the most extensively studied and validated one (Remer et al., 2008; Levy et al., 2010; He et al., 2017). The MODIS sensor observe the earth from 700 km altitude with $\pm 55^\circ$ view scan, having a swath of about 2330 km and covering nearly the entire globe in every 1 to 2 days, with 16 days of repeat cycle. It employs three separate operational algorithms for retrieving aerosol properties over land and oceans: the Dark Target (DT) algorithm over land, the DT algorithm over ocean and the Deep Blue (DB) algorithm over land. Both collection 5 (C5) and 5.1 DT and DB algorithms have been evaluated extensively on the regional scale (Li et al., 2007; Sayer et al., 2014), over IGP (Bilal et al., 2016) and on the global scale (Remer et al., 2008; Levy et al., 2010). The evaluation of MODIS Collection 6 (C6) data is still limited (Sayer et al., 2014; Bilal and Nichol, 2015; Nichol and Bilal, 2016). Recently launched C6 products contain refinements in terms of retrieving high radiometric quality of MODIS top-of-atmosphere (TOA) radiance and observations of reported contextual biases of the previous algorithms (Levy et al., 2010; Shi et al., 2013). Additionally, in order to recognize the aerosol climatology in a finer scale, a new daily global DT AOD data product with 3 km spatial resolution (MYD04_3K; Remer et al., 2013) is available in addition to standard DT (Levy et al., 2013) and DB (Hsu et al., 2013) AOD at 10 km resolution. The 3 km DT product is expected to perform better, especially in severely polluted atmosphere and for identifying exposure gradients over urban regions (Remer et al., 2013; He et al., 2017). To date, very few attempts were performed to evaluate the 3 km AOD products on a global scale (Remer et al., 2013), in urban/semi-urban regions (Munchak et al., 2013), and over specific regions (He et al., 2017; Nichol and Bilal, 2016; Ma et al., 2016). All these studies emphasized the need to evaluate the new product for other geographical regions. Further, C6 is also unique in merging scientific data sets (SDS) by including a 'best of' both DT and

DB (merged DT-DB) AOD products at 10 km resolution for all geographical regions, even for brighter surfaces like desert where DT is unable to retrieve AOD (Levy et al., 2013; Bilal and Nichol, 2015; Sorek-Hamer et al., 2015). However, all these data sets require explicit validation with respect to ground observation due to varying aerosol loading, aerosol sub-types, and land surface reflectance before being explicitly used in air pollution studies.

The present comparative analysis of MODIS aerosol products was made over the Indo-Gangetic Plain (IGP) in South Asia considering existing diversity of aerosol types and aerosol loading that prevails throughout the year (Fig. 1). The region is especially unique in terms of having diverse aerosols that varies over the seasons (Sen et al., 2017; Sayer et al., 2014) and has most often been associated with an aerosol induced impact on climate change (Ramanathan and Feng, 2009), agriculture and food security (Burney and Ramanathan, 2014), human health (Apte et al., 2015; Chowdhury and Dey, 2016) and thereby on sustainability of the region (Banerjee et al., 2017a, 2017b). Additionally, retrieval of high quality aerosol information is often challenging mainly due to significant inter-seasonal variation in surface reflectance across the IGP. Presence of dense vegetation with/without dark or bright soil surface, variation in aerosol SSA by influence of severe dust storms especially during pre-monsoon, and presence of fine particles especially during post-monsoon to winter, also induce uncertainties in retrieval of AOD (Tripathi et al., 2005; Bilal and Nichol, 2015). Therefore, recognizing the necessity of assessing the MODIS C6 products for its appropriateness in retrieving varying aerosols loading and aerosol types across IGP, and specifically for evaluating the MODIS C6 3 km DT products; this study provides a first comparative analysis of MODIS C6 DB at 10 km, DT at 3 and 10 km and merged SDS at 10 km (merged DT-DB) against each other and against the Aerosol Robotic Network (AERONET) ground-truth data available over the IGP for the years 2006 to 2015. Even, the study employs a broader perspective by evaluating AOD data by considering varying aerosol loading ($\text{AOD} < 0.3$; $0.3\text{--}1.2$ and > 1.2) and aerosols sub-types (Angstrom Exponent, $\alpha < 0.7$; $0.7\text{--}1.3$; > 1.3), thus accounting for vast aerosol heterogeneity that prevails over the region. Emphases are also made to recognize the retrieval uncertainty within different seasons and to compare the spatiotemporal uncertainties among the products. To our understanding, such comparative analysis of MODIS C6 AOD products including the DT at 3 km and merged DT-DB are reported for the first time over IGP, and will help potential end users to identify the appropriate database for retrieving AOD over the region.

2. Study domain, data set and methods

2.1. Description of the study domain

Among the globally identified major aerosol hotspots, IGP is often considered to be the most diverse in terms of particulate compositions and properties (Mhawish et al., 2018; Sen et al., 2017; Kumar et al., 2015b). Satellite based images of the global distribution of aerosol loading clearly identifies this region as most distinct due to the prevalence of high AOD throughout the year with considerable seasonality. The region typically spread across most of the northern and eastern India, Pakistan, and virtually all of Bangladesh (Fig. 1). Being a tropical to sub-tropical region, IGP also experiences deep convective layer, which occasionally lift fine aerosols to elevated atmosphere, thereby increased its residence time. Emissions from fossil fuel combustions are the most dominating source of fine particulates over IGP, followed by industrial emissions, secondary particulate formation and natural sources (Singh et al., 2017a). In contrast, coarser particulates originate mostly from re-suspensions of crustal materials (Banerjee et al., 2015). The physio-chemical and thereby, optical characteristics of aerosols are extremely diverse over the IGP (Singh et al., 2017a), with aerosols predominately of anthropogenic in nature during winter (December–February) and post-monsoon seasons (September–November).

These aerosols are composed primarily of organics that are emitted from biomass burning and vehicular emissions (Rajput et al., 2011; Kumar et al., 2017a; Singh et al., 2017b). In contrast, minerogenic crustal materials predominate during summer (pre-monsoon, March–May) and in monsoon (June–August; Tripathi et al., 2007; Murari et al., 2016, 2017). Further, the region is susceptible to airborne particulates of trans-boundary origin, primarily from middle-east Asia and central and western dry regions of India, which result in additional regional aerosol heterogeneity (Sen et al., 2016, 2017; Kumar et al., 2015b, 2017a). The comparison of Aqua MODIS retrieved AOD and ground data were made especially over the AERONET sites located across IGP, like in Karachi and Lahore (Pakistan); Gual Pahari (urban station close to New Delhi), Kanpur and Gandhi College (India) and Dhaka (Bangladesh). Detailed individual site characteristics may be found in the works of Bilal and Nichol (2015, Karachi and Lahore), Hyvärinen et al. (2011, Gual Pahari), Nichol and Bilal (2016, Kanpur and Gandhi College), Tripathi et al. (2005, Kanpur), and Singh et al. (2017a, 2017b).

2.2. AEROSOL ROBOTIC NETWORK (AERONET) AOD products

The AERONET is a global, ground-based network of calibrated Sun photometers (Holben et al., 1998) which provide cloud screened and quality assured spectral AOD within a range of 0.340 to $1.060\ \mu\text{m}$ (Smirnov et al., 2000) in every 15 min with a very low level of uncertainty ($0.01\text{--}0.02$). This ground-based aerosol network provides long-term, continuous and high-accurate spectral properties of aerosols, and was therefore extensively applied to validate satellite-based observations retrieved from various sensors (Li et al., 2007; Sayer et al., 2014; Bilal and Nichol, 2015; He et al., 2017). For the validation of the MODIS AOD products, AERONET Level 2.0 quality assured cloud screened data were collected every 15 min within 1 h of the MODIS overpass time over all the available stations across the IGP, namely Karachi (24.87°N , 67.03°E), Lahore (31.54°N , 74.32°E), Gual Pahari (28.43°N , 77.15°E), Kanpur (26.51°N , 80.23°E), Gandhi College (25.87°N , 84.13°E) and Dhaka (23.73°N , 90.40°E , Fig. 1, Table 1). Selection of AERONET sites across the IGP was made based on availability of minimum one-year level 2.0 AOD data, to recognize seasonal variations. Aqua MODIS AOD was also spatially averaged over each AERONET site for collocated observations. Ground-based AERONET AOD retrieved at $500\ \text{nm}$ were further interpolated to $550\ \text{nm}$ using the Angstrom power law, with wavelength pair of 440 to $675\ \text{nm}$. The SSA at wavelength 440 , 675 , 870 and $1020\ \text{nm}$ used in this study was obtained from AERONET Level 2 version 2 inversion algorithm, which is cloud screened and quality assured product (Dubovik and King, 2000; Dubovik et al., 2002). Information on aerosol size distribution ($\alpha_{440\text{--}870}$) is retrieved from AERONET Level 2.0 Version 2 Direct Sun Algorithm. The angstrom exponent (α) gives information on the distribution of aerosol size in the atmosphere. Low α (< 0.7) indicates larger particles, like dust, α within 0.7 to 1.3 indicates mixture of coarse and fine aerosols, and $\alpha > 1.3$ is typically characteristic of fine aerosols (Sayer et al., 2014). The single scattering albedo (SSA), defined as the ratio of scattering to total extinction, varies from 0 (purely absorbing aerosols) to 1 (purely scattering aerosols). The spectral dependence of SSA gives information on the abundance of light absorbing and scattering aerosols in the atmosphere.

2.3. Aqua MODIS AOD products

Algorithms used to retrieve AOD from MODIS on board Aqua and Terra satellites have most frequently updated to make use of improved knowledge on cloud-masking processes, aerosol models, and the surface reflectance throughout the globe. Recently released MODIS C6 has several advantages over C5 and C5.1, including additional availability of AOD products at a $3\ \text{km}$ resolution. For the present analysis, daily overpass time ($\sim 13:30$ local time, $\pm 60\ \text{min}$) mean Aqua-MODIS C6

Table 1
Summary of data sets used for the comparative analysis from 2006 to 2015.

File Name	SDS	Discription	Resolution & QA
AERONET	Aerosol Optical Depth (V2) & AE (α) Single Scattering Albedo(SSA)	Version 2 Direct Sun Algorithm Version 2 Inversion Algorithm	Data considered: Karachi (2006–14), Lahore (2007–15), Gual Pahari (2008–10), Kanpur (2006–15), Gandhi College (2006–15) and Dhaka (2012–15)
MYD04_3K	Optical_Depth_Land_and_Ocean	DT AOD at 550 nm over land and ocean	3 km QA = 3
MOD04_L2	Optical_Depth_Land_and_Ocean	DT AOD at 550 nm over land and ocean	10 km QA = 3
	Deep_Blue_Aerosol_Optical_Depth_550_Land_Best_Estimate	DB AOD at 550 nm over land	10 km QA > 2
	AOD_550_Dark_Target_Deep_Blue_Combined	Combined DT, DB AOD at 550 nm	10 km
	AOD_550_Dark_Target_Deep_Blue_Combined_Algorithm_Flag	for land and ocean	QA for DT = 3, DB > 2
		Combined Dark Target, Deep Blue AOT at 0.55-micron Algorithm Flag	

AOD at 550 nm with recommended quality assurance (QA) for DB at 10 km, DT at 3 km and 10 km and merged DT-DB at 10 km are simultaneously considered. All these products are principally based on three algorithms: the DT algorithm over land (Kaufman et al., 1997; Levy et al., 2013) and DT algorithm over ocean (Tanré et al., 1997), and the enhanced DB algorithm over land (Hsu et al., 2013).

The MODIS DB algorithm was originally developed to retrieve AOD at 10 km resolution over bright surfaces using deep blue wavelength (470 and/or 412/650 nm, depending on surface type), assuming location and season specific aerosol optical model (Sayer et al., 2013). The DB algorithm retrieve aerosol in cloud-free and snow-free pixels at nominal 1 km spatial resolution before aggregating it into 10 km resolution products. This is in contrast to the DT algorithm, which actually retrieves aerosol after aggregating radiance to 10 km. The “second generation” C6 version of the DB product has been further updated by Hsu et al. (2013) considering an improved assessment of NDVI-dependent surface reflectance, improved cloud screening and identification of dust. This helped to extend the applicability of the DB algorithm from arid/desert region to the entire land surface except for snow/ice covered areas. The expected error (EE) of the DB algorithm over land is reported as $\pm (0.05 + 20\%)$ (Hsu et al., 2013; Sayer et al., 2013).

The MODIS C6 DT algorithm in C6 has better assumptions than the C5 algorithm, especially in terms of updated cloud mask, thin-cirrus cloud and detection of heavy smoke. The C6 DT algorithm consists of two separate AOD products with different resolutions: 3×3 km and 10×10 km, both at Level 2. The DT algorithm was originally developed for dark vegetated surface area, where measured TOA reflectance at 500 m resolution is initially corrected for absorption by various gases before being organized within a 10×10 km (400 pixels, for 10 km) or a 3×3 km (36 pixels, for 3 km) retrieval box. The pixels are then processed to remove cloud, desert, snow/ice, inland water and the darkest 20% and brightest 50% pixels over land are arbitrarily deselected. Finally, at most 11 (for 3 km) and 120 (for 10 km) pixels remain to perform the aerosol retrieval by averaging their spectral reflectance. The inversion continues identically for the 3 km and the 10 km products based on combination of fine and coarse mode aerosol models (Remer et al., 2013). The DT algorithm at both 3 km and 10 km resolution was developed using identical aerosol inversion methods, LUT (Look-up table), surface reflectance and scattering angle. Yet, DT at 3 km is reported to be noisier compared to 10 km products (Munchak et al., 2013; Remer et al., 2013). The LUT in DT C6 assigns a moderately-absorbing fine-mode dominated aerosol to the IGP region (SSA ~ 0.91 at 550 nm) for all seasons except winter, while a strongly-absorbing fine-mode dominated aerosol (SSA ~ 0.87 at 550 nm) is only assigned to winter. In contrast, LUT in DT C6 only considers a single coarse model weakly absorbing aerosol (SSA ~ 0.95 at 550 nm) over the IGP region (Levy

et al., 2013). The DT 10 km aerosol products were evaluated extensively over the global (Levy et al., 2013) and the regional scales (Bilal et al., 2016; Bilal and Nichol, 2015; He et al., 2017), with a reported expected error (EE) over land of $\pm (0.05 + 15\%)$ (Levy et al., 2013). The DT 3 km aerosol products were evaluated both on the global (Remer et al., 2013) and the regional scales (He et al., 2017; Nichol and Bilal, 2016), with a reported expected error (EE) over land of $\pm (0.05 + 20\%)$ (Remer et al., 2013).

However, DT over land is not designed to retrieve AOD over bright surfaces while it is considered more accurate compared to DB (in C6) over dense vegetation (Levy et al., 2013). Furthermore, both DT and DB algorithms exclude snow-covered surfaces but have potential to be applied for all vegetated/transition areas with variable brightness. Therefore, a ‘best-of’ MODIS AOD products for all the transition regions was further included in the C6 as merged DT-DB AOD (AOD_550_Dark_Target_Deep_Blue_Combined) which is developed considering DT over vegetated/dark-soiled land, DT over ocean, and DB over desert/arid land (Levy et al., 2013). This is essentially developed considering a map of climatology data from MODIS NDVI product to determine the priority algorithm for retrieving AOD (Levy et al., 2013). In case the NDVI for a given month of specific area < 0.2 the algorithm selects DB AOD, and in case the NDVI > 0.3 , DT AOD are selected. For NDVI between 0.2 and 0.3, the higher quality of both DT and DB AOD is selected, or in case of both DT (QA = 3) and DB (QA ≥ 2), the mean of both AOD is considered. Recently, Bilal et al. (2017) have validated the merged DT-DB AOD product at global scale, and proposed a method independent of NDVI, for increasing the spatial coverage and decreasing the error. However, the merged DT-DB AOD still requires extensive regional validation. Considering the spatio-temporal variation of vegetation coverage and surface reflectance over the IGP, it seems that the merged DT-DB product has better applicability over the region, and therefore considered for comparison against AERONET.

2.4. Methodology

For the present analysis, Aqua-MODIS C6 AOD at 550 nm with recommended quality assurance (QA) for DB at 10 km (corresponding to retrievals flagged QA ≥ 2), DT at 3 and 10 km (retrievals flagged QA = 3) and merged DT-DB at 10 km products are simultaneously considered. The MODIS AOD was retrieved over AERONET sites within a sampling window with 3×3 pixels centred on the AERONET site. In order to increase the number of collocations between AERONET AOD and MODIS AOD, the average AERONET AOD measurement, obtained daily within ± 60 min of Aqua overpass time (approximately $\sim 13:30$ local time) is considered. To identify the spatial and temporal accuracy of MODIS retrieval against AERONET, all the collocated AOD

observations across the IGP, regardless of the retrieval algorithm were considered (N: 14,736). However, in order to study the effect of aerosol loading and type on the MODIS retrieval accuracy, a matched collocation between all the four MODIS products for same day and location were considered (N: 2416). To compare the performance of individual algorithms, the criteria proposed by Sayer et al. (2014) that the performance difference should exceeds some threshold (0.1 in R, 0.1 in EE, 20% in number of collocation or 0.03 in RMSE) was used.

The statistical tools and techniques which were used for quantifying the accuracy and precision of the different MODIS algorithms in retrieving AOD are: an orthogonal regression technique ($Y = a + bX$) used to estimate the slope (b) and intercept (a) between MODIS AOD ($AOD_{(MODIS)}$) and AERONET AOD ($AOD_{(AE)}$). The intercept is used as an indicator of uncertainty of the surface reflectance estimation, and the slope is associated with the error in the assumptions of the aerosol model. The correlation coefficient (R), root mean squared error (RMSE, Eq. (1)), mean absolute error (MAE, Eq. (2)), relative mean bias (RMB, Eq. (3)), and the expected error (EE, Eq. (4)) have been further used to evaluate the retrieval accuracy.

$$RMSE = \sqrt{\frac{1}{n} \sum_{i=1}^n (AOD_{(MODIS)i} - AOD_{(AE)i})^2} \quad (1)$$

$$MAE = \frac{1}{n} \sum_{i=1}^n |AOD_{(MODIS)i} - AOD_{(AE)i}| \quad (2)$$

$$RMB = \frac{1}{n} \sum_{i=1}^n \left| AOD_{(MODIS)i} / AOD_{(AE)i} \right| \quad (3)$$

$$EE = \pm (0.05 + 0.15AOD_{AE}) \quad (4)$$

3. Results and discussion

3.1. Evaluation of MODIS retrieval accuracy against AERONET

The MODIS Collection 6 AOD products like DT AOD at 3 km resolution, DT AOD at 10 km, DB AOD at 10 km and merged DT-DB AOD at 10 km are plotted against AERONET AOD measured over six AERONET sites across IGP (Fig. 2, Table 2). A total of 14,736 collocated MODIS aerosol retrievals (AOD at 550 nm) spanning within year 2006 to 2015 with recommended QA are compared to recognize the quality of C6 aerosol retrieval accuracy over varying land surfaces reflectance and aerosol types. The number of collocation vary within the products with the merged DT-DB AOD having the highest collocation (N: 4360) over the IGP followed by DB AOD (N: 4059). The DT 3 km appears to have the lowest collocation (N: 2850) because of its inability to retrieve AOD over sparsely vegetated, dry and bright surfaces that are characterized by a very high surface reflectance (Levy et al., 2013). This reduced collocation of DT 3 km products over IGP is identical to previous findings over Asia (Bilal and Nichol, 2015; Nichol and Bilal, 2016; He et al., 2017) and global wise (Remer et al., 2013).

The evaluation of MODIS AOD was considered both in terms of the retrievals falling within the estimated uncertainty of one standard deviation from the average (Fig. 2a–d, Levy et al., 2010; Remer et al., 2013) and the distribution of MODIS AOD bias as a function of AERONET (Fig. 3). Both DT 10 km and 3 km resolutions appear to overestimate AOD by a margin of 14–25% (RMB, DT 10 km: 1.144; DT 3 km: 1.248) with 61.29% and 51.37% of retrievals falling within the EE, respectively. The DT 10 km provides a better agreement (R: 0.832) with AERONET AOD across the IGP, with comparatively lower RMSE (0.218), relative to the DT 3 km AOD (R: 0.743, RMSE: 0.280). Both C6 DT AOD products use similar aerosol inversion methods, LUT, and land surface reflectance, and are therefore expected to perform identically. However, the larger intercept of DT 3 km (0.122) compared to DT 10 km (0.062) indicates higher uncertainties in estimating the surface

reflectance at visible wavelength. The DT AOD at both 3 km and 10 km resolutions show positive bias at low and high AOD values. Overall, the DT AOD 10 km outperformed in term of retrievals falling within the EE, and the bias tends to be positive for both low and high AOD values (RMB: 1.144), indicating errors in selection of the aerosol model. The DT 3 km showed lower performance and higher positive bias than DT 10 km, signifying underestimation of the surface reflectance, which is similar to the observations reported by Remer et al. (2013), Nichol and Bilal (2016) and He et al. (2017). The DB 10 km AOD product represent almost similar agreement with AERONET (R, DB: 0.83; DT: 0.83) but has larger N, poorer retrieval accuracy (EE, DB: 53.76%; DT: 61.29%), almost identical RMSE (0.214) and largely underestimated AOD (RMB: 0.825) as compared to AOD by DT 10 km (RMB: 1.144). The DB AOD also shows negative bias at all AOD values (Fig. 3), while at low AOD the negative bias indicates the overestimation of surface reflectance. In contrary, at high AOD values, the DB shows significant negative bias which is due to the effect of overestimation of the surface reflectance and aerosol SSA (Sayer et al., 2014). Overall, the DB algorithm underestimated AOD while the DT algorithm overestimated AOD, suggesting that both have limitations in estimating the surface reflectance and in selecting appropriate aerosol model across the IGP (Bilal et al., 2016). The merged DT-DB AOD also exhibits a poor performance, with 56.03% retrievals falling within the EE, an equivalent MAE (0.153), and RMB close to one (1.002). In principal, since the merged product combines DB, DT-land and DT-ocean, it increases the spatial coverage of the individual algorithms over dark and bright surfaces. Further, due to the opposing bias of DT and DB, the merged AOD showed about zero mean bias at low AOD values and mostly a negative bias at high and very high AOD values. Namely, in spite of the fact that the merged DT-DB AOD product is dominated by DT AOD, the negative bias at high and very high AOD is due to the significant negative bias of the DB AOD and the DT AOD bias tend to be negative at very high AOD values. Nonetheless, the merged DT-DB AOD product does not meet the requirements of the EE (= 68%). In fact, all the MODIS AOD products failed to achieve the target of 68% retrievals within the EE bound in comparison to AERONET. This led us to examine the spatial variation of the retrieval accuracy of each product.

3.2. Spatial variation of retrieval accuracy of MODIS AOD products

In order to understand the spatial variation of the retrieval accuracy of different MODIS algorithms, MODIS AOD products with AERONET AOD for the six stations across the IGP were compared.

3.2.1. Evaluation of DT 3 km (MYD04_3 km) AOD

Fig. 4 shows the comparison between DT 3 km and AERONET AOD across the IGP while the distribution of the DT 3 km AOD bias as a function of the AERONET AOD is depicted in Fig. S1 (Supplementary Information). It is evident that the performance of DT 3 km is site specific and mainly depends on the surface characteristics and the dominating aerosol type over each site (Table S1). The overall agreement of DT 3 km with AERONET is positive and significant ($R \geq 0.8$) throughout the IGP except for Dhaka (R: 0.5), which is located at the lower IGP. DT 3 km fails to retrieve AOD especially over highly bright surfaces like Karachi, with very few collocations (N: 56) compared to the same algorithm at a lower spatial resolution (DT 10 km, N: 471). Karachi is urban build up area with much bare land, which is dominated by mixed type of aerosols such as coarse minerogenic materials, marine and anthropogenic aerosols (Singh et al., 2017a; Bilal et al., 2016). Over Karachi, 98.21% of the retrievals fall above the EE, and the high positive bias of the DT 3 km AOD retrievals at low and high AOD values (Fig. S1) indicates underestimation of the surface reflectance as well as uncertainty in selection a proper aerosol model.

Over the rest of IGP (western part of upper IGP, middle and lower IGP), with relatively darker land surface and dominated by either mixed (coarse and anthropogenic aerosol) and/or fine (industrial pollutions

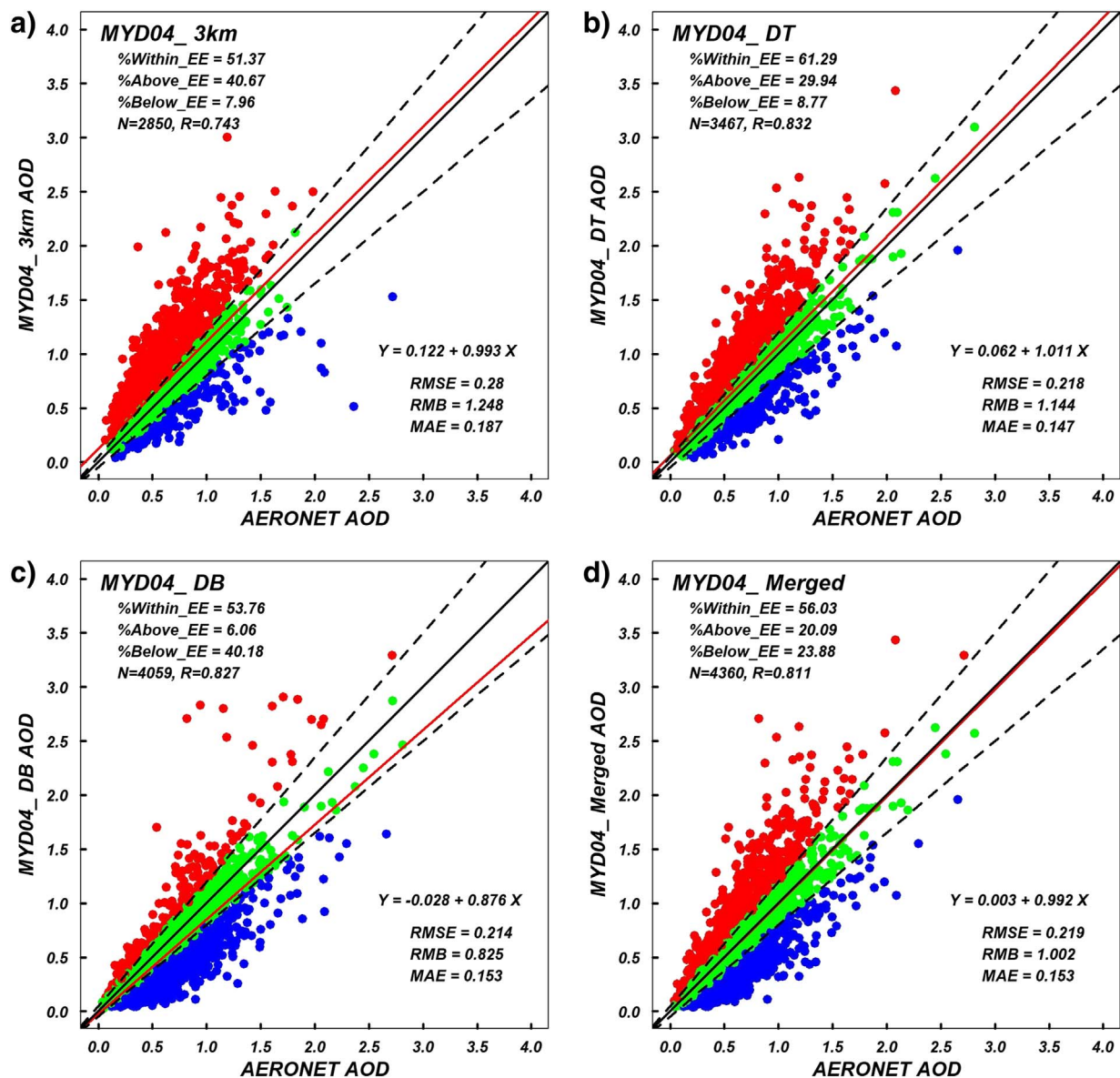


Fig. 2. Evaluation of Aqua MODIS (a) DT 3 km, (b) DT 10 km, (c) DB 10 km and (d) merged DT-DB 10 km AOD against AERONET AOD for all sites across IGP from 2006 to 2015. The red solid line represents regression line, the dash lines are the EE lines, and the black solid line is 1:1 line. The red, green and blue dots represent the collocation points falling above, within and below the EE. (For interpretation of the references to colour in this figure legend, the reader is referred to the web version of this article.)

and smoke) mode aerosols, the DT 3 km performs better. Over both the urban cities of Lahore and Kanpur, the DT 3 km showed significant overestimation of AOD. The DT 3 km retrievals significantly overestimated AOD over Lahore (RMB: 1.488), with only 29.40% of the retrievals falling within the EE. The retrieval accuracy over Kanpur is comparatively better (% within EE: 57.34) than in Lahore, with lower RMB (1.261). This is mainly due to higher uncertainty in the estimation of the surface reflectance over Lahore compared to Kanpur, which is evident by having higher bias at low AOD. Further, the highest AOD retrieval uncertainty is mainly evident during coarse dominating

aerosol episodes in the monsoon season. Over Gual Pahari, the DT 3 km shows good agreement with AERONET AOD ($R: 0.854$), with 63.64% of collocations falling within the EE. However, the DT 3 km underestimated the AOD over Gual Pahari (RMB: 0.916). Dhaka, a typical Asian megacity that is located at the lower IGP and is dominated by fine absorbing aerosols throughout the year (Singh et al., 2017a). The retrieval of DT 3 km AOD over Dhaka showed almost zero mean bias at low AOD, while for increased AOD the retrievals tend to result a more negative bias, indicating low absorption in the selected aerosol models, especially during the winter and post-monsoon. The decrease in SSA

Table 2

Evaluation summary of DT 3 km, DT 10 km, DB 10 km, and merged DT-DB 10 km AOD products against AERONET AOD over the IGP region for the years from 2006 to 2015.

Algorithm	N	AOD	AOD _{AE}	R	RMSE	RMB	MAE	= EE %	> EE%	< EE%
DT 3 km	2850	0.704	0.586	0.743	0.280	1.248	0.187	51.37	40.67	7.96
DT 10 km	3467	0.653	0.584	0.832	0.218	1.144	0.147	61.29	29.94	8.77
DB 10 km	4059	0.468	0.567	0.827	0.214	0.825	0.153	53.76	6.06	40.18
merged DT-DB	4360	0.566	0.568	0.811	0.219	1.002	0.153	56.03	20.09	23.88

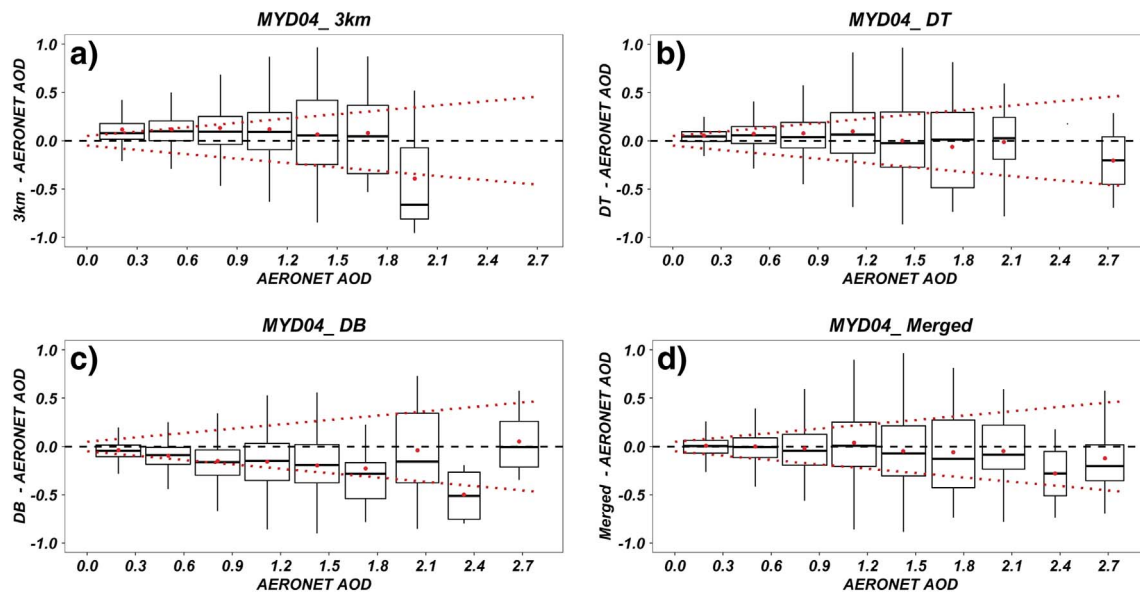


Fig. 3. Box plot of Aqua MODIS (a) DT 3 km, (b) DT 10 km, (c) DB 10 km and (d) merged DT-DB 10 km AOD bias against AERONET AOD. The black horizontal dashed line represents zero bias and the red dotted lines represent the EE. For each box, the middle line, red dot, upper and lower hinges represent the AOD bias median, mean, 25th and 75th percentiles, respectively. The whiskers extend to 1.5 times the interquartile range (IQR). (For interpretation of the references to colour in this figure legend, the reader is referred to the web version of this article.)

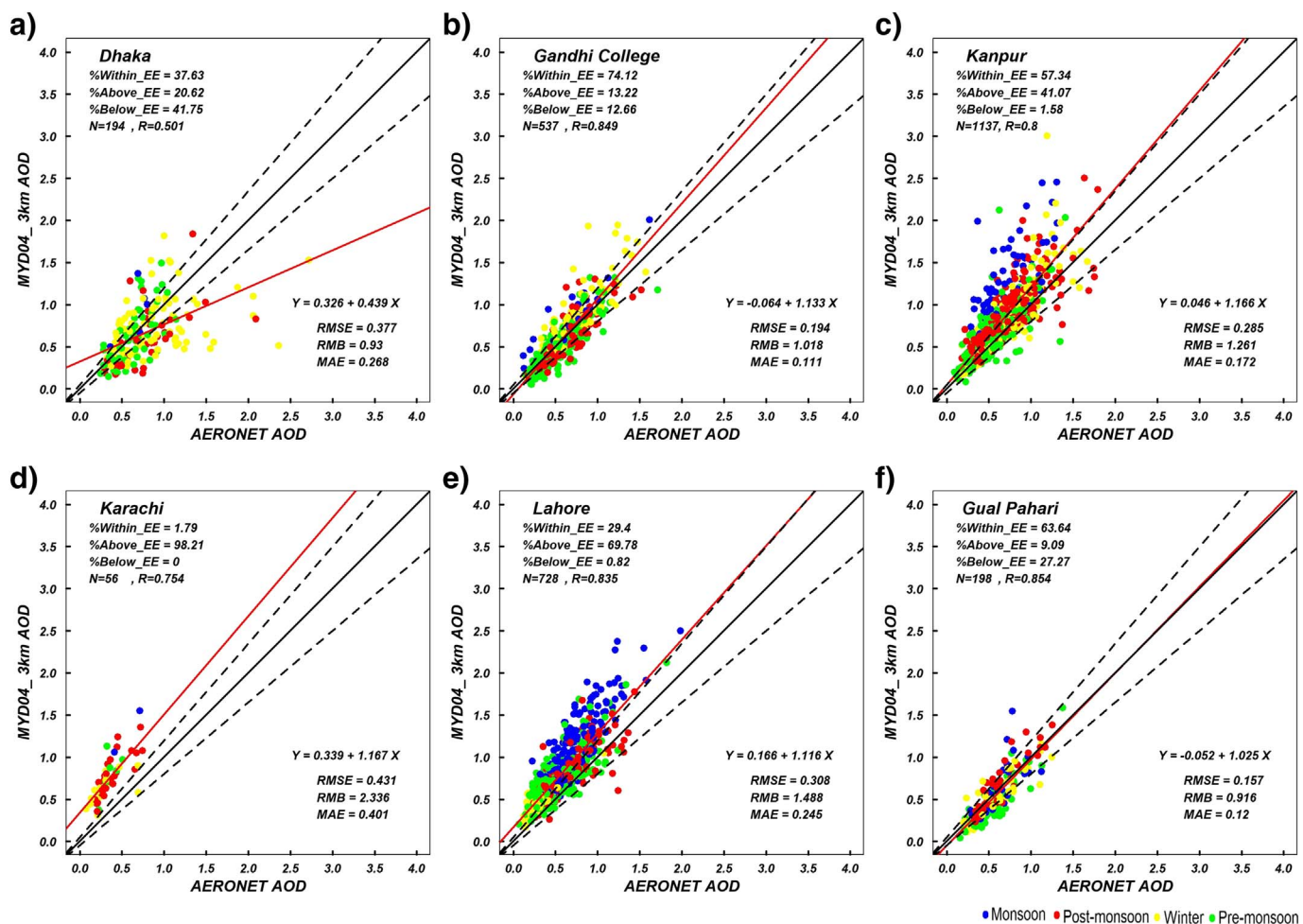


Fig. 4. Evaluation of Aqua MODIS DT 3 km AOD against AERONET AOD at (a) Dhaka (b) Gandhi college (c) Kanpur (d) Karachi (e) Lahore (f) Gual Pahari. The red solid line represents regression line, the dash lines are the EE lines, and the black solid line is 1:1 line. (For interpretation of the references to colour in this figure legend, the reader is referred to the web version of this article.)

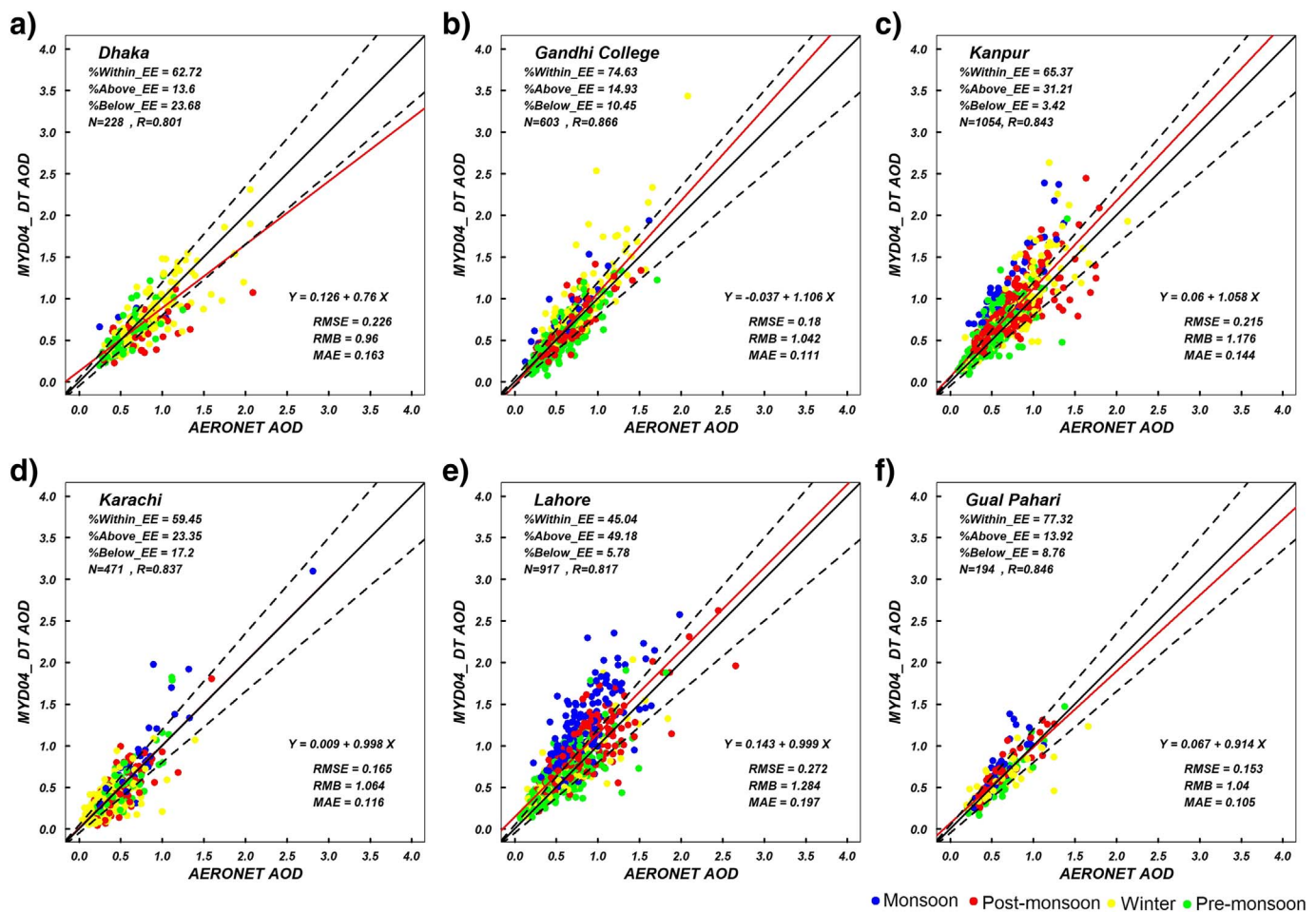


Fig. 5. Evaluation of Aqua MODIS DT 10 km AOD against AERONET AOD at (a) Dhaka (b) Gandhi college (c) Kanpur (d) Karachi (e) Lahore (f) Gual Pahari. The red solid line represents regression line, the dash lines are the EE lines, and the black solid line is 1:1 line. (For interpretation of the references to colour in this figure legend, the reader is referred to the web version of this article.)

with increasing wavelength indicates the abundance of absorbing aerosols (e.g. BC) in the fine and mixed dominated aerosol (Table S2). The SSA is affected by high BC loading from vehicular emissions, household energy practices and waste/biomass burning. Furthermore, DT 3 km performed poorly over Dhaka also in terms of having only 37.63% of the observation within the EE, revealing a high RMSE (0.377), and the poorest agreement (R: 0.501) with AERONET AOD. The Gandhi college, a rural site over the middle IGP, is characterized by vegetation and green coverage and the aerosol profile is dominated by coarse particles during pre-monsoon, mixed type particles during monsoon, and by fine particles in the post-monsoon and winter (Table S2). DT 3 km performed very well at this site as the algorithm is especially tuned towards dark (vegetated) surfaces. The DT 3 km retrieved AOD over Gandhi college with 74.12% falling within the EE, showing low RMB (1.018), RMSE (0.194) and MAE (0.111). Overall, as shown in Table S1, retrievals of AOD by DT 3 km varies within region and the algorithm does succeed to identify spatial variation. Overall, the DT 3 km failed to achieve satisfactory AOD retrievals over urban cities like Lahore and Kanpur having positive bias compared to AERONET AOD and negative bias over Dhaka. In general, the DT 3 km failed to achieve satisfactory AOD retrievals across the IGP except in Gandhi college, and exhibited poor performance compared to DT 10 km throughout the IGP.

3.2.2. Evaluation of DT 10 km (MYD04_L2) AOD

Overall, the DT 10 km product shows better agreement with AERONET ($R \geq 0.8$) across the IGP, with improved retrieval accuracy

and collocated observation (N: 3467) compared to DT 3 km (N: 2850). The number of retrievals by the DT 10 km algorithm is considerably higher compared to DT 3 km, especially over bright surfaces like Karachi (N, DT 10 km: 471, 3 km: 56) (Fig. 5). The highest disagreement between these two algorithms occurs especially over the bright surfaces like in Karachi. The retrieval accuracy of DT 10 km over brighter surfaces is significantly higher (% within EE: 59.45) compared to DT 3 km, while the mean bias decreased from 2.336 (RMB, DT 3 km) to 1.064 (RMB, DT 10 km). The uncertainty in the estimation of the surface reflectance by DT 10 km (bias at low AOD) over urban area is smaller compared to that obtained by DT 3 km (Fig. S2). This is mainly due to the elimination of bright pixels in the deselection process within a larger retrieval box (10×10 km), which are possibly selected during the 3 km deselection process. Thus, the DT 3 km is considered to be noisier compared to the DT 10 km product (Remer et al., 2013). Overall, the DT 10 km product outperformed DT 3 km across IGP, particularly over urban areas.

The retrieval accuracy of DT 10 km was better than of DT 3 km over two urban areas, Lahore (% within EE: 45.04) and Kanpur (% within EE: 65.37). Over Lahore, DT 10 km is found to overestimate AOD (RMB: 1.284) compared to Kanpur (RMB: 1.176). Similar to the DT 3 km, the positive bias of DT 10 km at low AOD values (< 0.5) was higher over Lahore than over Kanpur, indicating underestimation of the surface reflectance over both sites but more severely over Lahore. In contrast, the underestimation of the AOD over Dhaka suggests large uncertainty in selecting the aerosol model, which shows negative bias at high AOD values. Nevertheless, the DT 10 km outperformed the 3 km with

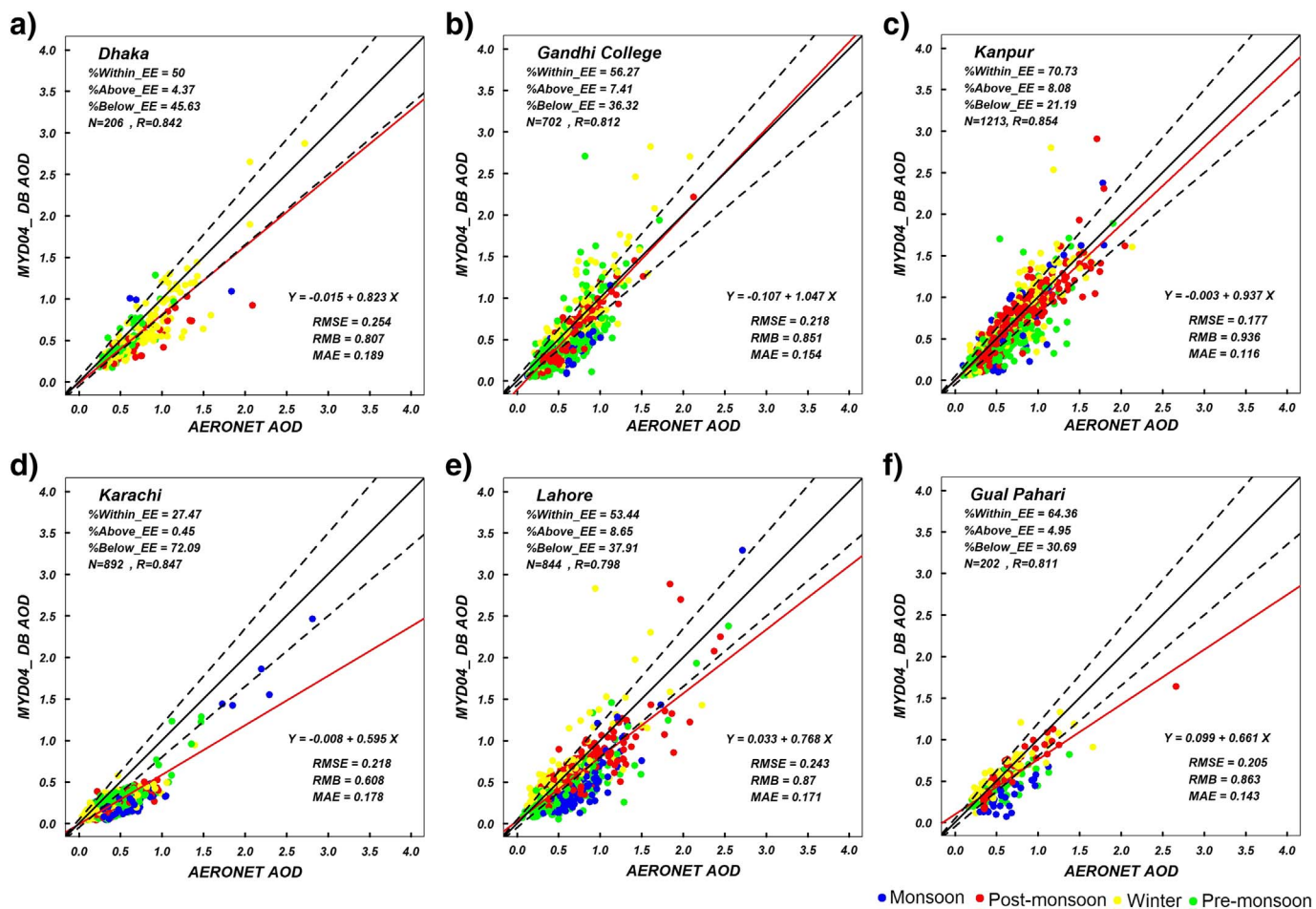


Fig. 6. Evaluation of Aqua MODIS DB 10 km AOD against AERONET AOD at (a) Dhaka (b) Gandhi college (c) Kanpur (d) Karachi (e) Lahore (f) Gual Pahari. The red solid line represents regression line, the dash lines are the EE lines, and the black solid line is 1:1 line. (For interpretation of the references to colour in this figure legend, the reader is referred to the web version of this article.)

62.72% of the retrieval falling within the EE compared to the DT 3 km (37.63%). The DT 10 km product performed satisfactorily over Gual Pahari (% within EE: 77.32) and Gandhi college (% within EE: 74.63), showing relatively low bias (RMB: 1.04 and 1.042, respectively) and RMSE (0.153 and 0.18, respectively). Conclusively, the DT 10 km algorithm is found to perform better than the DT 3 km, but to generally overestimate the AOD across the IGP.

3.2.3. Evaluation of DB 10 km (MYD04_L2) AOD

Fig. 6 shows comparison of DB 10 km AOD against AERONET AOD. The MODIS C6 DB algorithm was expected to retrieve AOD over both arid/desert region and vegetated surfaces, even during low aerosol conditions (Hsu et al., 2013). The DB AOD has a total collocation of N: 4059 across the IGP, with station specific collocation well comparable to the merged DT-DB product. Moreover, it also appears to have a good agreement ($R \geq 0.8$) with AERONET, with overall underestimation of AOD by 6–40% (RMB: 0.608–0.936) over all the AERONET sites across the IGP.

Interestingly, in comparison to DT 10 km, the number of collocation over bright areas like Karachi has almost doubled (N: 892) but with more than two third of these points falling below the EE (% within EE: 27.47). The significant underestimation of DB 10 km AOD for all aerosol conditions (Fig. S3) indicates a considerable overestimation of the surface reflectance and of the aerosol SSA for coarse mode aerosol dominated regions. Our findings are similar to those reported in previous studies (Sayer et al., 2014; Bilal et al., 2016) over Karachi. The performance of DB 10 km considerably improved over Lahore (RMSE:

0.243; MAE: 0.171) and Kanpur (RMSE: 0.177; MAE: 0.116), with 53.4% and 70.73% of the collocations falling within the EE. Further, relatively low bias at low AOD indicates that the estimation of surface reflectance is comparatively better in the DB than in the DT algorithms, especially over Lahore which showed large positive bias at low AOD. The increasing negative bias with AOD values in both cities indicates that the aerosol model lacks absorbing particles, especially over Lahore. Additionally, the scatterplots (Fig. 6) show that the most of retrieved AOD during fine aerosols dominated seasons (post-monsoon and winter) fall within the estimated error. Likewise, during post-monsoon and winter, improved retrieval accuracy was achieved for both Lahore (% within EE: 60–76%) and Kanpur (72–77%), while retrieval accuracy deteriorates during dominance of coarser aerosols in monsoon and pre-monsoon (Lahore: 18–48% and Kanpur: 52–68%). Interestingly, in spite of having almost identical AE (0.64–1.26) and SSA (0.86–0.91), DB 10 km performs differently over Lahore and Kanpur. This may possibly due to low absorption in aerosol model over Lahore, as with the increase in AOD, the negative bias increases sharply over Lahore in comparison to Kanpur, suggesting an overestimated surface reflectance and/or overestimated aerosols SSA. Nonetheless, the DB retrieval accuracy over Lahore is the best among all the other algorithms although it failed to achieve the targeted EE to be considered successful aerosol retrieval. In contrast, DB 10 km AOD performed satisfactorily over Kanpur owing to 70.73% of its AOD retrievals falling within the EE.

Over Dhaka, both the DT and the DB algorithms significantly underestimated the AOD (RMB: 0.807, % within EE: 50.0), which could be explained by overestimation of the SSA by the aerosol model. The DB

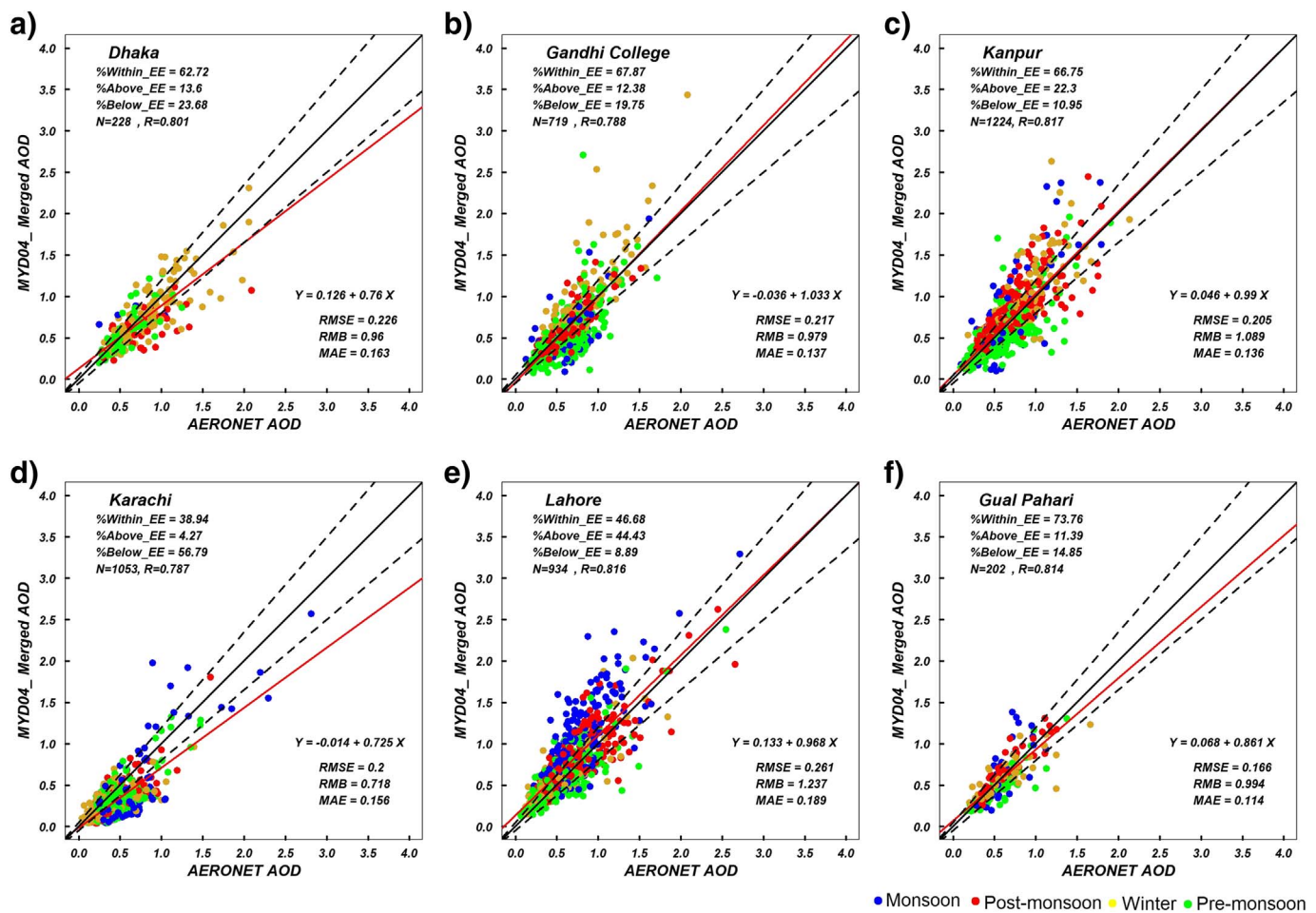


Fig. 7. Evaluation of Aqua MODIS merged DT-DB 10 km AOD against AERONET AOD at (a) Dhaka (b) Gandhi college (c) Kanpur (d) Karachi (e) Lahore (f) Gual Pahari. The red solid line represents regression line, the dash lines are the EE lines, and the black solid line is 1:1 line. (For interpretation of the references to colour in this figure legend, the reader is referred to the web version of this article.)

Table 3

Contribution of DT and DB AOD to the merged DT-DB AOD over the six AERONET stations across the IGP from 2006 to 2015.

Site	Total Merged AOD	DT contribution	DB contribution	Mixed (mean DT & DB)
Karachi	2060	636 (30.8%)	1425 (69.2%)	0
Lahore	2274	2009 (88.3%)	99 (4.4%)	331 (7.3%)
Gual Pahari	2110	1577 (74.7%)	235 (11.1%)	298 (14.2%)
Kanpur	1946	1434 (73.7%)	387 (19.9%)	249 (6.4%)
Gandhi college	1888	1382 (73.2%)	310 (16.4%)	196 (10.4%)
Dhaka	1308	1308 (100%)	0	0

10 km AOD achieved poor performance also over the rural station of Gandhi College (% within EE: 56.27) and over the semi-urban station of Gual Pahari (% within EE: 64.36), which is surrounded by vegetation. In comparison to DT 10 km, DB 10 km performed poorly over both stations and considerably underestimated the AOD (RMB, Gandhi College: 0.851, Gual Pahari: 0.863), primarily due to overestimating of the SSA of the coarser particles (Sayer et al., 2014).

The DB 10 km showed negative bias in retrieving AOD for all the stations over IGP especially during coarse aerosols dominated pre-monsoon and monsoon seasons, while in case of Dhaka and Karachi, the negative bias was persistent throughout the year. Conclusively, the DB 10 km AOD significantly underestimated the AOD at all sites across the IGP regardless of the aerosol columnar loading, with RMB varying from

0.608 to 0.936. This indicates that the absorption in the aerosol models in the LUT needs to be modified over the IGP. However, it should be noted that AERONET observations are quite limited in some of the stations, in particular Gual Pahari and Dhaka, which may also contribute to the poor comparisons against the AERONET AOD.

3.2.4. Evaluation of merged DT-DB 10 km (MYD04_L2) AOD

Fig. 7 shows the comparison between the merged DT-DB 10 km AOD and AERONET AOD at the six sites across the IGP. In principle, the uncertainty of the merged AOD product depends on the relative contribution of DT 10 km and DB 10 km AOD. The overall trend of the DT algorithm across the IGP is to overestimate AOD while the DB algorithm is generally found to underestimate the AOD. Thereby, the merged product is expected to overestimate AOD in the region that is dominated by DT retrievals and to underestimate AOD where DB retrievals dominate. Table 3 shows the relative contribution of the DT and DB algorithms to the merged product for 10 years of data across the IGP. Merged retrievals are found to be dominated by DT, with contribution varying from 73 to 100% (except for Karachi, 31%). Overall, the merged product exhibits better agreement with the AERONET AOD ($R \geq 0.8$) with higher collocated retrievals compared to the other algorithms and lower bias.

Over Karachi, the general trend of AOD retrieval by the merged product is to underestimate the AOD (RMB: 0.718), with 38.94% retrieval accuracy within the EE. Due to the relatively bright land surface (NDVI < 0.2), the merged DT-DB used the DB 10 km product (69%) over Karachi, while for the rest of the IGP the trend is almost reversed.

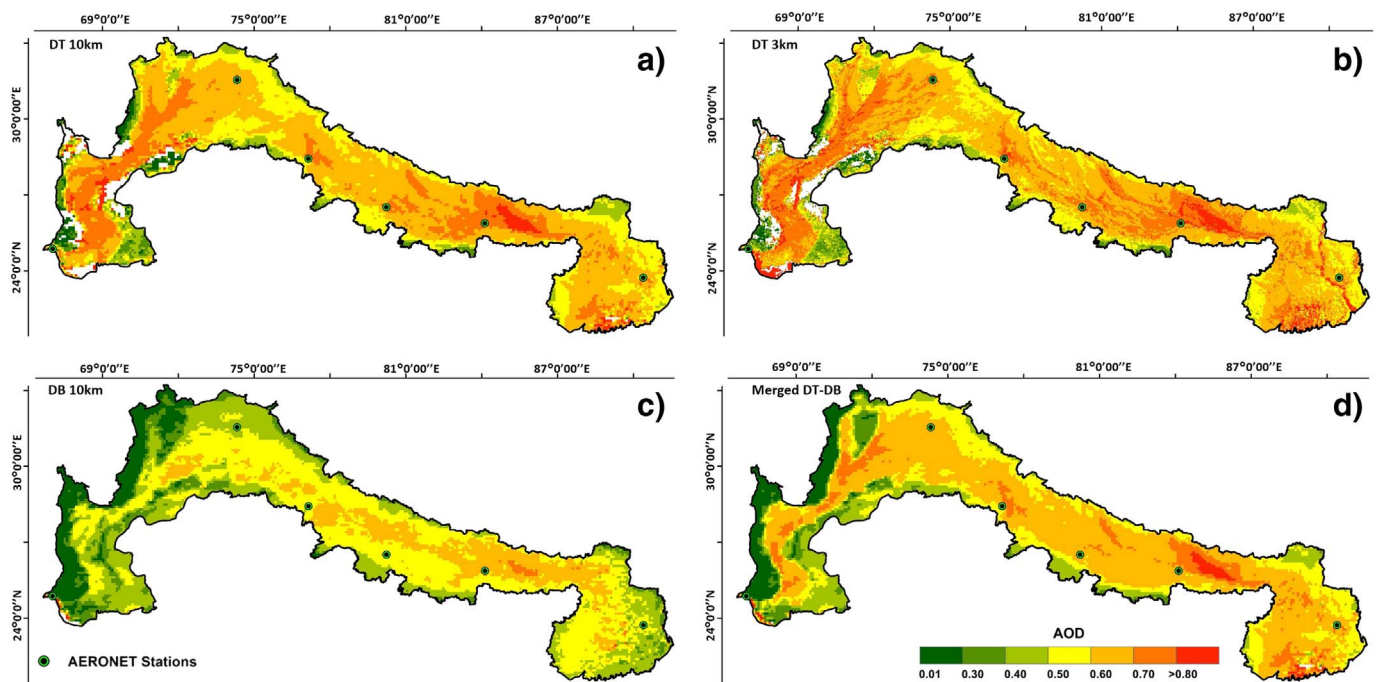


Fig. 8. Spatial distribution of 10 years (2006–2015) average AOD over the IGP for (a) DT 10 km, (b) DT 3 km, (c) DB 10 km and (d) merged DT-DB.

The retrieval accuracy slightly improves over Lahore (% within EE: 45.68; RMB: 1.237) relative to DT 3 km (29.4%, 1.488) while the performance is almost identical to DT 10 km (45.04%, 1.284) and inferior to the DB 10 km (53.44%, 0.870) AOD products. Furthermore, as the merged DT-DB product follows completely the DT 10 km over Dhaka (%within EE: 62.72), the retrieval statistics match exactly those of the DT 10 km (Fig. 5). In Gual Pahari and Gandhi College, the merged DT-DB AOD is almost similarly dominated by DT retrievals (73–75%), produced identical results with minor underestimation of the AOD (RMB: 0.979–0.994), and had satisfactory retrieval accuracy within EE (68–74%). Over Kanpur, the merged product showed relatively lower bias than DT 10 km and identical retrieval accuracy (% within EE: 66.75%). In summary, the merged product improves the spatial coverage over the IGP and reduces the bias due to the opposing DT and DB bias.

Fig. 8 explains the geographical distribution of AOD across IGP retrieved by all four MODIS C6 algorithms from 2006 to 2015. Both DT, DB and merged products appear to have varying level of uncertainties in retrieving AOD over varying land surfaces. It is clear that the DT 10 km retrievals have more missing/no data pixels across IGP, particularly over Baluchistan region (upper IGP) compared to DB 10 km, with 10,442 pixels (97.2%) available for DT 10 km compared to 10,732 for DB (99.9%). The Baluchistan region is mostly dry and bright having very high surface reflectance (Fig. 1) with dominance of coarser airborne particulates. DT algorithm excludes pixels with surface reflectance > 0.25 in the mid-infrared channel ($2.12 \mu\text{m}$) and also discards 50% of the brightest and 20% of the darkest pixels, therefore it was expected to retrieve less number of pixels over these surfaces (Levy et al., 2013). Further, within upper IGP, DT especially failed to retrieve over low AOD condition with sparsely vegetated surfaces upon bright land mass. Further, both DT (3 and 10 km) and DB 10 km AOD retrievals exhibit different spatial pattern in columnar aerosol with comparatively high AOD retrieved by DT with a multiyear average of 0.697 for DT 10 km and 0.704 for DT 3 km, across IGP. In contrast, DB recognized a slightly reduced spatial variation of columnar aerosols with a multiyear average AOD of 0.502. Multi-year mean difference between these two AOD products varies differently over IGP and 80% of differences lies within < 0.20 .

3.3. Temporal variation of retrieval accuracy

The retrieval accuracy of MODIS AOD over the IGP indicates considerable temporal variation within seasons. The fundamental reason behind the intra-seasonal variation is varying aerosol loading across the IGP. Seasonal variation results from changing synoptic pattern in meteorological conditions that affect in aerosol optical and microphysical properties, as well as from changes in the surface reflectance due to vegetation growth phases, especially agricultural crops.

Fig. 9 shows the seasonal variation in aerosol size distribution (Angstrom Exponent α) and spectral dependencies of SSA obtained from AERONET measurements across the IGP. The pre-monsoon and monsoon seasons over IGP show domination of coarse mode aerosol with α ranging from ~ 0.3 (over Karachi) to 0.68 (over Gandhi college, Table S2) except over Dhaka, which reported a higher α ($\alpha > 1$) throughout the seasons. The SSA found to increase with wavelength over all sites (except Dhaka) due to dominated coarse scattering particles in the atmosphere. The high α value and decreasing SSA with wavelength over Dhaka can be attributed to dominating fine and absorbing aerosol types over all the seasons.

Table 4 shows the seasonal variation of AOD retrieval accuracy for the four MODIS AOD products in comparison to AERONET AOD. The performance of the MODIS retrieval algorithms was relatively improved during pre-monsoon compared to the monsoon season. During pre-monsoon conditions, DT 10 km is found to perform satisfactorily, overestimating AOD by only 8% (RMB: 1.082) and with 69.75% of the retrievals falling within the EE range. Moreover, the number of collocations was somewhat lower for DT 10 km (N: 1167) in comparison to the merged DT-DB (N: 1630) and the DB 10 km (N: 1552) algorithms, showing higher agreement with the AERONET AOD (R: 0.813) and can undoubtedly be considered as the best product during pre-monsoon.

The highest uncertainty of all MODIS AOD products is found during the monsoon months, with RMSE varying from 0.361 to 0.494 among the AOD products (Fig. S2, in supplementary file). The monsoon season experiences the lowest number of collocation for all the products (11% of total collocations) due to extended cloud coverage. All algorithms show a significant deviation in retrieving AOD during monsoon, with 22.12% to 32.71% of the retrievals falling within the EE. Both resolutions of DT and the merged DT-DB products indicate significant

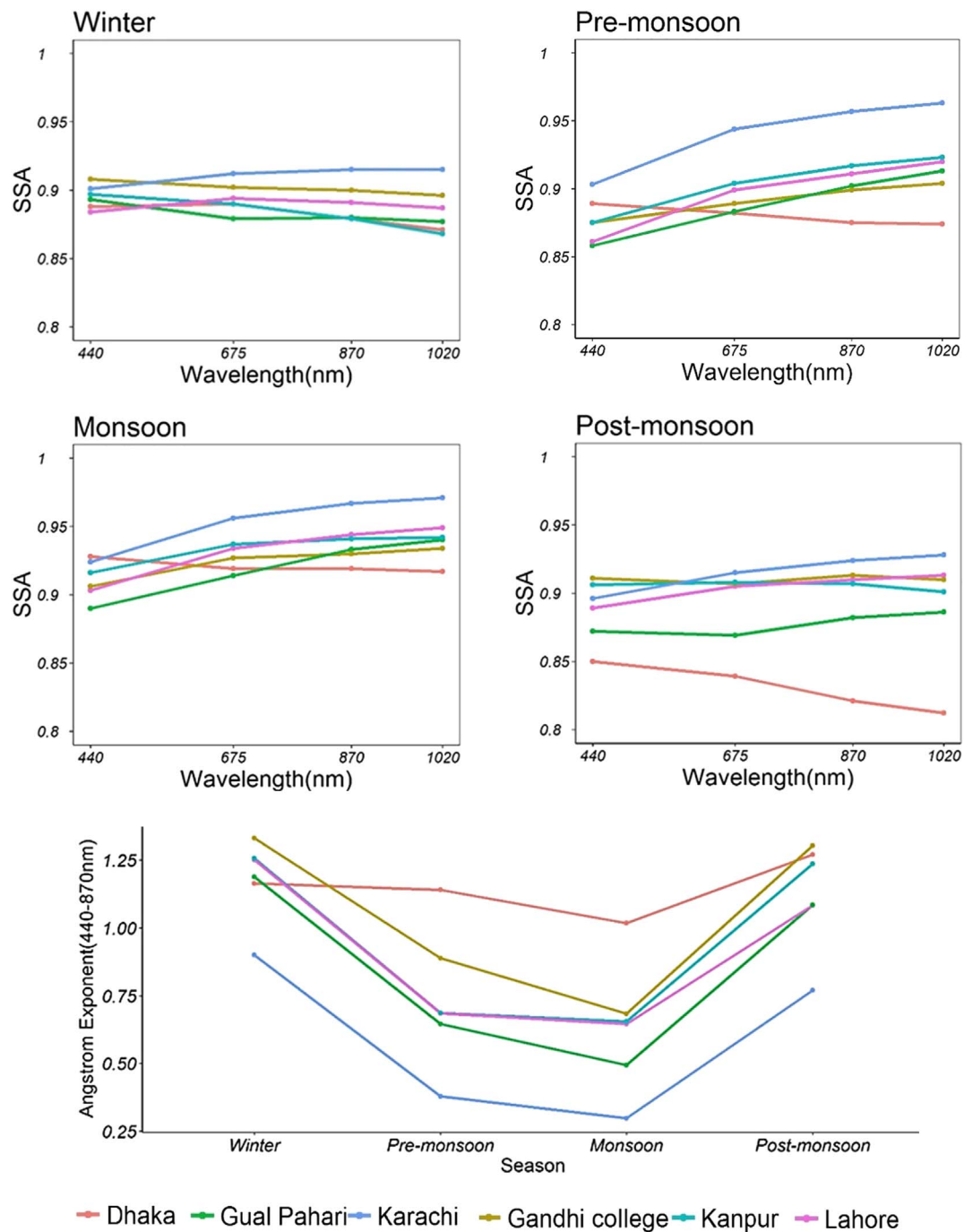


Fig. 9. Variations of seasonal mean spectral SSA (440 to 1020 nm) and Angstrom Exponent (440 to 870 nm) over the six AERONET stations during winter, pre-monsoon, monsoon and post-monsoon.

overestimation of AOD and poor retrieval accuracy. The largest disagreements between the DT (RMB: 1.447) and DB (RMB: 0.644) algorithms are found during the monsoon, where DT 10 km results in 44.7% overestimation in AOD and DB 10 km results in 35.6% underestimation. The high dissimilarity between DB and DT AOD in the monsoon season has been in accordance to Sayer et al. (2014) and Bilal et al. (2016).

Slight increase in the SSA with wavelength and increase in α during winter suggest the presence of mixed-size absorbing aerosols over the upper IGP (Karachi and Lahore). The AERONET stations over middle and lower IGP exhibit decrease in SSA with wavelength during winter and increase in α , indicating dominance of absorbing fine mode aerosols. During post-monsoon, the spectral dependence of SSA is low over all sites across IGP except Dhaka, indicating the presence of mixed

aerosol (Dubovik et al., 2002). Over Dhaka, the lower and high spectral dependence of the SSA is due to the presence of high absorbing aerosol types in the atmosphere. Both during post-monsoon and winter, not even a single AOD algorithm emerged to have satisfactory performance. However, the overall trends are similar, with the DB under predicting the AOD by 7–16% and the DT 10 km overestimating the AOD by 12–13%. The merged DT-DB product follows the behavior of the DT algorithm and overestimates the AOD in all seasons except pre-monsoon. In all the seasons, the merged product achieved the lowest bias in comparison to either DT or DB products due to the tendency of the DB to underestimate and of the DT to overestimate the AOD when compared to ground-truth measurements. The high temporal variation in AOD retrieval accuracy across the IGP indicates the associated

Table 4

Seasonal summary of error statistics for the DT 3 km, DT 10 km, DB 10 km, and merged DT-DB 10 km AOD products against AERONET AOD over the IGP.

Algorithm	Season	N	$\alpha_{440-870}$	R	RMSE	RMB	MAE	: EE%	> EE%	< EE%
DT 3 km	Premonsoon	1078	0.786	0.766	0.196	1.181	0.143	58.35	32.10	9.55
	Monsoon	330	0.613	0.745	0.494	1.582	0.383	22.12	76.06	1.82
	Post-monsoon	760	1.161	0.750	0.265	1.249	0.188	45.79	46.18	8.03
	Winter	682	1.247	0.753	0.268	1.192	0.159	60.7	30.94	8.36
DT 10 km	Premonsoon	1167	0.697	0.813	0.157	1.082	0.110	69.75	20.65	9.60
	Monsoon	363	0.505	0.814	0.401	1.447	0.317	31.13	67.49	1.38
	Post-monsoon	912	1.095	0.836	0.200	1.122	0.148	58.33	32.02	9.65
	Winter	1025	1.149	0.864	0.201	1.128	0.130	64.98	25.37	9.66
DB 10 km	Premonsoon	1552	0.774	0.765	0.206	0.785	0.151	52.96	2.84	44.20
	Monsoon	368	0.597	0.826	0.311	0.644	0.269	24.18	4.89	70.92
	Post-monsoon	1021	1.124	0.877	0.191	0.843	0.134	59.84	5.00	35.16
	Winter	1118	1.177	0.857	0.204	0.925	0.134	59.03	11.90	29.07
Merged DT-DB	Premonsoon	1630	0.699	0.751	0.188	0.930	0.134	60.18	11.10	28.71
	Monsoon	483	0.543	0.740	0.361	1.131	0.282	32.71	41.61	25.67
	Post-monsoon	1067	1.079	0.832	0.202	1.015	0.154	51.27	25.49	23.24
	Winter	1180	1.134	0.872	0.193	1.036	0.125	64.15	18.81	17.03

uncertainties within all the AOD algorithms in selecting appropriate aerosol model and surface reflectance. This led us to further examine the retrieval accuracy of each algorithm for different aerosol loading and aerosol type conditions across IGP and discussed in following section.

3.4. Comparison of MODIS AOD products against AERONET: Influence of aerosol loading and types

Previously, we compared MODIS AOD products against ground-truth measurement obtained by six AERONET stations that are distributed across the IGP. The results indicated that the all the algorithms vary in their retrieval performance metrics. The retrieval accuracy was found to vary considerably in terms of both the spatial and temporal scales. Accounting for the aerosol heterogeneity across the IGP, the performance of each algorithm is further evaluated with respect to the varying aerosol loading (in terms of AOD) and the dominant particle size (Table 5). For this, only the matched collocations (N: 2416) between all algorithms were used. The collocated AERONET AOD (AOD_{AE}) was divided into three subsets based on the aerosol loading. For the first subset, scenarios with low aerosol loading ($AOD_{AE} < 0.3$) are used to examine the contribution of the surface reflectance to the AOD retrievals. Next, two cases are examined: relatively high ($0.3 < AOD_{AE} < 1.2$) and very high aerosol loading ($AOD_{AE} > 1.2$). These scenarios are used for evaluating the effects of varying aerosol size on the performance of aerosol retrieval algorithm. The aerosol loading scenarios, except for the low loading condition ($AOD_{AE} < 0.3$), are further complicated by considering the dominance of aerosol types and explored to identify the best retrieval algorithm for each case. Angstrom Exponent (α , Fig. 9) over the wavelength range of 440 to 870 nm is retrieved from AERONET Level 2 to determine the relative dominance of fine or coarse mode aerosols in the atmosphere (Eck et al., 1999; Reid et al., 1999). Subsequently, three aerosol type scenarios are considered: (1) coarse particles (e.g. dust, $\alpha < 0.7$), (2) mixed mode (e.g. mixture of coarse and fine aerosols, $0.7 < \alpha < 1.3$), and (3) fine particles (e.g. mainly anthropogenic-like industrial emissions, biomass burning, etc., $\alpha > 1.3$).

Since the contribution of aerosol to the TOA reflectance is small in low AOD scenarios ($AOD_{AE} < 0.3$; Levy et al., 2013), the estimation of the surface reflectance by MODIS algorithms is possible. Results show that the DT 10 km, DB 10 km and merged DT-DB 10 km algorithms performed almost equally in terms of retrieval accuracy ($\sim 67\%$). The dissimilarity between these algorithms is in the bias, likewise DT 3 km and DT 10 km algorithms showed positive bias at low AOD conditions, which indicates that the algorithms underestimate the surface reflectance across the IGP. Such an underestimation of the surface

reflectance also induces overestimation of the retrieved AOD (RMB, DT 3 km: 1.446, DT 10 km: 1.255) with only 51.74 and 66.56% of the collocations falling within the EE, respectively. The lower bias of DT 10 km compared to DT 3 km also indicates the better estimates of the surface reflectance by DT 10 km. In contrast, under the same conditions the DB algorithm shows low negative bias that induces small underestimation of the retrieved AOD (RMB: 0.976) across the IGP, which indicates better estimation of the surface reflectance. However, in spite of underestimating AOD, the DB 10 km AOD retrieval process outperformed other algorithms and achieved a satisfactory retrieval accuracy (% within EE: 68.77), with a low deviation of RMB from unity. The merged DT-DB AOD showed lower positive bias at low AOD value as it underestimated the surface reflectance across the IGP, overestimating the AOD (RMB: 1.234) and obtaining 67.51% of retrieval accuracy. As the merged product mainly follows the DT algorithm across the IGP (Table 5), underestimation of surface reflectance was expected.

Fig. 10 shows the distribution of the AOD bias as a function of aerosol size ($\alpha_{440-870}$) for high aerosols loading conditions ($AOD_{AE} > 0.3$). The distribution of the bias across the range of particles gives an idea of the dependency of the retrieval accuracy on aerosol particle size. For DT 3 km and 10 km AOD, the relative bias tends to remain large and positive for coarse mode aerosols and low and positive for fine particle dominated aerosol. However, the extent of variation is smaller for DT 10 km than for DT 3 km AOD, signifying that the retrieval accuracy of DT 10 km has lower sensitivity for varying particle size. This results in almost comparable retrieval accuracies for DT 10 km and 3 km AOD for varying particle size, although DT 3 km retrievals appear to be noisier (Remer et al., 2013) and to have larger uncertainty in the surface reflectance estimation throughout IGP (Nichol and Bilal, 2016). In contrast, the DB 10 km AOD shows large negative bias for coarse particle dominated scenarios and the bias tends to reduce significantly with the increase in the fine particles. This invariably suggests that the DB AOD bias has a larger dependence on the particle size. The merged AOD product shows very little bias in coarse-dominated aerosol type, the lowest among all other products, and the bias tends to be positive for mixed and fine-dominated aerosol.

Table 5 shows the error statistics of the four MODIS AOD for fine, mixed and coarse-dominated aerosol at high and very high aerosol loading. For fine-dominated aerosol, the DB performs the best among all other algorithms in terms of RMB (0.982), RMSE (0.134) and the fraction falling within the EE (76.02%). The DT 10 km performs better than DT 3 km for all aerosol types, and identically to the merged DT-DB AOD. For mixed-dominated aerosol all the algorithms performed identically within a threshold of 10% of EE and a correlation coefficient or a difference in the RMSE < 0.03 . For coarse mode aerosols the

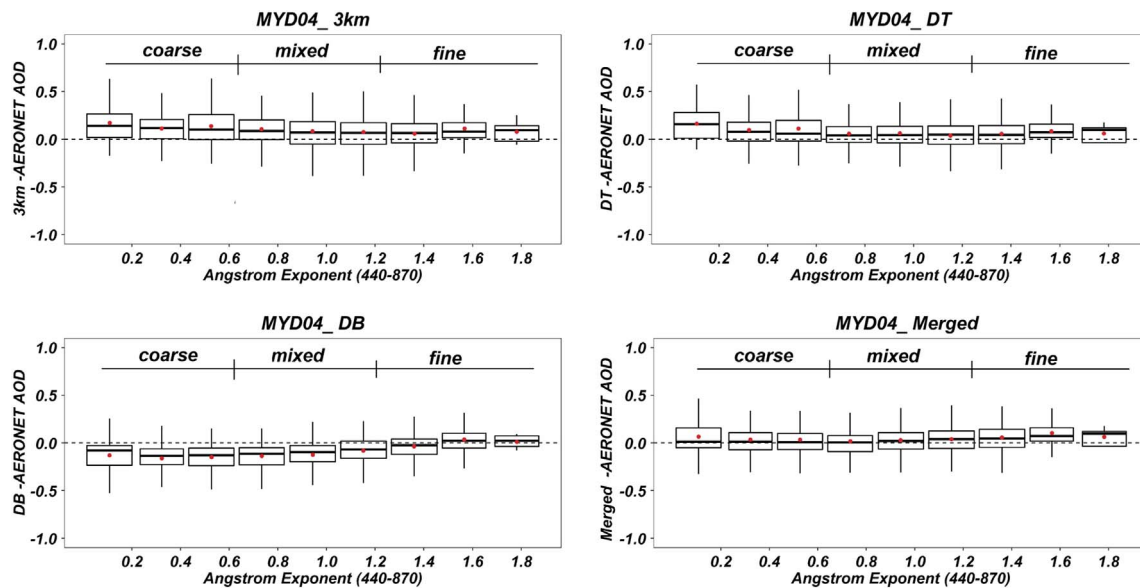


Fig. 10. Box plot of Aqua MODIS DT 3 km, DT 10 km, DB 10 km and merged DT-DB 10 km match up AOD bias (MODIS – AERONET AOD) as a function of AERONET angstrom exponent (α 440–870) over the IGP. The black horizontal dashed line represents zero bias.

- The DT 3 km, DT 10 km and merged DT-DB AOD overestimate the AOD across the IGP, with 51–61% of retrievals within the expected error envelope. They also exhibit significant spatio-temporal variation of the retrieval accuracy across the IGP. In comparison, the DB AOD consistently underestimates the AERONET AOD, with 54% retrieval accuracy within the expected error bounds. Conclusively, none of the C6 products appear to achieve the satisfactory retrieval accuracy within EE (68%) across the IGP while having considerable seasonality and geographic variability.
- The retrieval accuracy of C6 products was found to be strongly dependent on the surface characteristics and the aerosol type. The DT 3 km algorithm shows lower retrieval accuracy over all the urban-background sites, while over rural site it performed reasonably well. The DT 10 km algorithm outperformed the DT 3 km with a higher retrieval accuracy, especially over urban areas. Overall, the DT 3 km product is found to underestimate the surface reflectance more in comparison to the DT 10 km, and thereby to over predict the AOD across the IGP.
- The DB 10 km algorithm is able to retrieve AOD over arid/desert regions and vegetated areas even for low aerosol conditions, and generally underestimate the AOD over all the surface. In spite of the higher retrieval over bright surfaces, it significantly underestimates AOD due to overestimates of the surface reflectance and aerosol SSA, especially over coarse aerosol dominated region.
- Across IGP, the merged DT-DB product was found to be dominated by DT retrievals (73 to 100%) except over bright land surfaces, like in Karachi. In term of bias, the merged product shows lower bias over all the sites due to opposite tendency of DT (positive bias) and DB (negative bias). In terms of retrieval accuracy, it performed as good as the DT and DB products except over the upper IGP. Therefore, the merged product may be considered better suited for recognizing seasonality and/or aerosol sub-types across the IGP while it still lacks extended validation over heterogeneous land surfaces.
- MODIS products showed seasonal variations in retrieval number and accuracy due to the seasonal change in aerosol characteristics and NDVI throughout the IGP. The lowest retrieval number and accuracy was found during the monsoon season. DT 10 km had higher number and showed better accuracy during the pre-monsoon and winter, while DB retrievals were better during winter and post-monsoon periods.
- The retrieval accuracies are also compared in terms of varying aerosol loading (low, high and very high) and dominance of aerosol sub-types (fine, mixed and coarse) based on data from the six AERONET stations. For relatively cleaner environment ($AOD < 0.3$), DT at both resolutions overestimated the surface reflectance while DB better predicted the surface reflectance across the IGP and outperformed all the other algorithms in terms of achieving satisfactory retrieval accuracy and lower deviation of RMB from unity.
- The effect of high aerosols loading and size were diverse for different algorithms across IGP. For varying aerosol sizes, the retrieval accuracy of DT 10 km has lower sensitivity while DT 3 km appears to have large uncertainty in estimating the surface reflectance. In contrast, DB 10 km exhibits larger dependence of the bias on the particle size, and it has the best performance among all the other algorithms for fine-dominated aerosols. For mixed aerosol scenarios, all the algorithms performed almost identically within the threshold level. For coarse aerosols, the merged DT-DB AOD and the DT 10 km product outperformed the DB and DT 3 km algorithms with the merged AOD appearing to have lower RMSE and satisfactory retrieval accuracy.
- In the case of $AOD_{AE} > 1.2$ and dominant fraction of fine and mixed aerosols, all the algorithms except DT 3 km performed almost equally in terms of retrieval accuracy, RMB and RMSE. When absorbing aerosols are dominant (e.g. BC and mineral dust), DB undoubtedly agrees better with AERONET although there is an indication of error in the aerosol models in all the algorithms. For a large fraction of coarse aerosols, the disagreement between the DB and DT retrievals increases, and none of the algorithms except the merged DT-DB product showed satisfactory performance.
- Based on our results, we conclude that DB is more accurate in retrieving fine mode aerosols while DT 10 km algorithm shows an almost identical performance when retrieving all aerosol size. The merged DT-DB AOD was found to have higher accuracy for coarse-dominated aerosol conditions, when the dissimilarity between DT and DB is highest.

Acknowledgments

The MODIS data used in this study are available at Atmosphere Archive & Distribution System (LAADS) (<https://ladsweb.nascom.nasa.gov>).

gov/search/), and the AERONET products at <https://aeronet.gsfc.nasa.gov/>. D.B. acknowledges the generous support of the Leona M. and Harry B. Helmsley Charitable Trust to the Technion-Shantou University Collaboration in Environmental Health (Grant# 2015PG-ISL006) and financial support from the Ministry of Science and Technology, Israel (Grant # 3-13142). S.T. acknowledges partial support from the Department of Science and Technology, Govt. of India under the DST-UKEIRI (DST/INT/UK/P-144/2016). We would like to thank the Principal Investigators for establishing and maintaining AERONET sites over IGP.

Appendix A. Supplementary data

Supplementary data to this article can be found online at <https://doi.org/10.1016/j.rse.2017.09.016>.

References

- Apte, J.S., Marshall, J.D., Cohen, A.J., Brauer, M., 2015. Addressing global mortality from ambient PM_{2.5}. *Environ. Sci. Technol.* 49, 8057–8066.
- Banerjee, T., Murari, V., Kumar, M., Raju, M.P., 2015. Source apportionment of airborne particulates through receptor modeling: Indian scenario. *Atmos. Res.* 167–187.
- Banerjee, T., Kumar, M., Mall, R.K., Singh, R.S., 2017a. Airing ‘clean air’ in Clean India Mission. *Environ. Sci. Pollut. Res.* 24, 6399–6413.
- Banerjee, T., Kumar, M., Singh, N., 2017b. Aerosol, climate and sustainability. In: Reference Module in Earth Systems and Environmental Sciences. Encyclopaedia of Anthropocene. Elsevier. <http://dx.doi.org/10.1016/B978-0-12-409548-9.09914-0>.
- Bilal, M., Nichol, J.E., 2015. Evaluation of MODIS aerosol retrieval algorithms over the Beijing-Tianjin-Hebei region during low to very high pollution events. *J. Geophys. Res. Atmos.* 120, 7941–7957. <http://dx.doi.org/10.1002/2015JD023082>.
- Bilal, M., Nichol, J.E., Nazeer, M., 2016. Validation of aqua-MODIS C051 and C006 operational aerosol products using AERONET measurements over Pakistan. *IEEE J. Sel. Topics Appl. Earth Obs. Remote Sens.* 9 (5), 2074–2080.
- Bilal, M., Nichol, J.E., Wang, L., 2017. New customized methods for improvement of the MODIS C6 dark target and deep blue merged aerosol product. *Remote Sens. Environ.* 197, 115–124.
- Boucher, R., Randall, A.D., Bretherton, P., Feingold, C., Forster, G., Kerminen, P., Kondo, V.M., Liao, Y., Lohmann, H., Rasch, U., Satheesh, P., 2013. Clouds and aerosols in climate change 2013. In: The Physical Science Basis. Contribution of Working Group I to the Fifth Assessment Report of the Intergovernmental Panel on Climate Change. Cambridge University Press Cambridge, United Kingdom and New York, NY, USA.
- Burney, J., Ramanathan, V., 2014. Recent climate and air pollution impacts on Indian agriculture. *Proc. Natl. Acad. Sci. U. S. A.* 111 (46), 16319–16324.
- Chen, W.T., Lee, Y.H., Adams, P.J., Nenes, A., Seinfeld, J.H., 2010. Will black carbon mitigation dampen aerosol indirect forcing? *Geophys. Res. Lett.* 37, L09801.
- Chowdhury, S., Dey, S., 2016. Cause-specific premature death from ambient PM_{2.5} exposure in India: estimate adjusted for baseline mortality. *Environ. Int.* 91, 283–290.
- Creamean, J.M., Suski, K.J., Rosenfeld, D., Cazorla, A., DeMott, P.J., Sullivan, R.C., White, A.B., Ralph, F.M., Minnis, P., Comstock, J.M., Tomlinson, J.M., 2013. Dust and biological aerosols from the Sahara and Asia influence precipitation in the western US. *Science* 339 (6127), 1572–1578.
- Dey, S., Tripathi, S.N., Singh, R.P., Holben, B.N., 2004. Influence of dust storms on the aerosol optical properties over the Indo-Gangetic basin. *J. Geophys. Res.* 109, D20211. <http://dx.doi.org/10.1029/2004JD004924>.
- Dubovik, O., King, M.D., 2000. A flexible inversion algorithm for retrieval of aerosol optical properties from sun and sky radiance measurements. *J. Geophys. Res.* 105, 20673–20696.
- Dubovik, O., Holben, B., Eck, T.F., Smirnov, A., Kaufman, Y.J., King, M.D., Tanré, D., Slutsker, I., 2002. Variability of absorption and optical properties of key aerosol types observed in world-wide locations. *J. Atmos. Sci.* 59, 590–608.
- Eck, T.F., Holben, B.N., Reid, J.S., Dubovik, O., Smirnov, A., O'Neill, N.T., Slutsker, I., Kinne, S., 1999. Wavelength dependence of the optical depth of biomass burning, urban, and desert dust aerosols. *J. Geophys. Res.* 104 (D24), 31,333–31,349.
- Fang, H., Liang, S., Hoogenboom, G., 2011. Integration of MODIS products and a crop simulation model for crop yield estimation. *Int. J. Remote Sens.* 32 (2011), 1039–1065.
- Gupta, R., Somanathan, E., Dey, S., 2017. Global warming and local air pollution have reduced wheat yields in India. *Clim. Chang.* 140, 593. <http://dx.doi.org/10.1007/s10584-016-1878-8>.
- He, Q., Zhang, M., Huang, B., Tong, X., 2017. MODIS 3 km and 10 km aerosol optical depth for China: Evaluation and comparison. *Atmos. Environ.* 153, 150–162.
- Holben, B.N., Eck, T.F., Slutsker, I., Tanre, D., Buis, J.P., Setzer, A., Vermote, E., Reagan, J.A., Kaufman, Y.J., Nakajima, T., Lavenu, F., 1998. AERONET—A federated instrument network and data archive for aerosol characterization. *Remote Sens. Environ.* 66 (1), 1–16.
- Hsu, N.C., Jeong, M.-J., Bettenhausen, C., Sayer, A.M., Hansell, R., Seftor, C.S., Huang, J., Tsay, S.-C., 2013. Enhanced deep blue aerosol retrieval algorithm: the second generation. *J. Geophys. Res. Atmos.* 118, 9296–9315. <http://dx.doi.org/10.1002/jgrd.50712>.
- Hyvärinen, A.P., Raatikainen, T., Komppula, M., Mielonen, T., Sundström, A.M., Brus, D., Panwar, T.S., Hooda, R.K., Sharma, V.P., Leeuw, G.D., Lihavainen, H., 2011. Effect of the summer monsoon on aerosols at two measurement stations in Northern India—part 2: physical and optical properties. *Atmos. Chem. Phys.* 11 (16), 8283–8294.
- Kahn, R., Gailley, B.J., Garay, M.J., Diner, D.J., Eck, T.F., Smirnov, A., Holben, B.N., 2010. Multiangle imaging Spectroradiometer global aerosol product assessment by comparison with the Aerosol Robotic Network. *J. Geophys. Res.* 115, D23209. <http://dx.doi.org/10.1029/2010JD014601>.
- Kaufman, Y.J., Wald, A.E., Remer, L.A., Gao, B.-C., Li, R.-R., Flynn, L., 1997. The MODIS 2.1 μ m channel-correlation with visible reflectance for use in remote sensing of aerosol. *IEEE Trans. Geosci. Remote Sens.* 35 (5), 1286–1298. <http://dx.doi.org/10.1109/36.628795>.
- Kaufman, Y.J., Koren, I., Remer, L.A., Tanre, D., Ginoux, P., Fan, S., 2005. Dust transport and deposition observed from the terramoderate resolution imaging spectro-radiometer (MODIS) spacecraft over the Atlantic Ocean. *J. Geophys. Res.* 110, 1–16.
- Kumar, M., Singh, R.S., Banerjee, T., 2015a. Associating airborne particulates and human health: exploring possibilities. *Environ. Int.* 84, 201–202.
- Kumar, M., Tiwari, S., Murari, V., Singh, A.K., Banerjee, T., 2015b. Wintertime characteristics of aerosols at middle Indo-Gangetic Plain: impacts of regional meteorology and long range transport. *Atmos. Environ.* 104, 162–175.
- Kumar, M., Singh, R.K., Murari, V., Singh, A.K., Singh, R.S., Banerjee, T., 2016. Fireworks induced particle pollution: a spatio-temporal analysis. *Atmos. Res.* 180, 78–91.
- Kumar, M., Raju, M.P., Singh, R.S., Banerjee, T., 2017a. Impact of drought and normal monsoon scenarios on aerosol induced radiative forcing and atmospheric heating in Varanasi over middle Indo-Gangetic Plain. *J. Aerosol Sci.* 113, 95–107.
- Kumar, M., Raju, M.P., Singh, R.K., Singh, A.K., Singh, R.S., Banerjee, T., 2017b. Wintertime characteristics of aerosols over middle Indo-Gangetic Plain: vertical profile, transport and radiative forcing. *Atmos. Res.* 183, 268–282.
- Levy, R.C., Remer, L.A., Kleidman, R.G., Mattoo, S., Ichoku, C., Kahn, R., Eck, T.F., 2010. Global evaluation of the Collection 5 MODIS dark-target aerosol products over land. *Atmos. Chem. Phys.* 10, 10399–10420. <http://dx.doi.org/10.5194/acp-10-10399-2010>.
- Levy, R.C., Mattoo, S., Munchak, L.A., Remer, L.A., Sayer, A.M., Patadia, F., Hsu, N.C., 2013. The Collection 6 MODIS aerosol products over land and ocean. *Atmos. Meas. Tech.* 6 (11), 2989–3034. <http://dx.doi.org/10.5194/amt-6-2989-2013>.
- Li, Z., Niu, F., Lee, K.H., Xin, J., Hao, W.M., Nordgren, B., Wang, Y., Wang, P., 2007. Validation and understanding of Moderate resolution imaging Spectroradiometer aerosol products (C5) using ground-based measurements from the handheld sun photometer network in China. *J. Geophys. Res. Atmos.* 112 (D22).
- Li, J., Carlson, B.E., Laci, A.A., 2014a. Application of spectral analysis techniques in the intercomparison of aerosol data. Part II: using maximum covariance analysis to effectively compare spatiotemporal variability of satellite and AERONET measured aerosol optical depth. *J. Geophys. Res. Atmos.* 119, 153–166.
- Li, J., Carlson, B.E., Laci, A.A., 2014b. Application of spectral analysis techniques in the intercomparison of aerosol data: part III. Using combined PCA to compare spatiotemporal variability of MODIS, MISR, and OMI aerosol optical depth. *J. Geophys. Res. Atmos.* 119, 4017–4042.
- Ma, Y., Li, Z., Li, Z., Xie, Y., Fu, Q., Li, D., Zhang, Y., Xu, H., Li, K., 2016. Validation of MODIS aerosol optical depth retrieval over mountains in Central China based on a sun-sky radiometer site of SONET. *Remote Sens.* 8 (2), 111.
- Mhawish, A., Kumar, M., Mishra, A.K., Srivastava, P.K., Banerjee, T., 2018. Remote sensing of aerosols from space: retrieval of properties and applications. In: *Remote Sensing of Aerosols, Clouds, and Precipitation*. Elsevier Inc, pp. 1–38. <http://dx.doi.org/10.1016/B978-0-12-810437-8.00003-7>.
- Munchak, L., Levy, R., Mattoo, S., Remer, L., Holben, B., Schafer, J., Hostetler, C., Ferrare, R., 2013. MODIS 3 km aerosol product: applications over land in an urban/suburban region. *Atmos. Meas. Tech.* 6 (7), 1747–1759.
- Murari, V., Kumar, M., Mhawish, A., Barman, S.C., Banerjee, T., 2017. Airborne particulate in Varanasi over middle Indo-Gangetic Plain: variation in particulate types and meteorological influences. *Environ. Monit. Assess.* 189, 157. <http://dx.doi.org/10.1007/s10661-017-5859-9>.
- Murari, V., Kumar, M., Singh, N., Singh, R.S., Banerjee, T., 2016. Particulate morphology and elemental characteristics: variability at middle Indo-Gangetic Plain. *J. Atmos. Chem.* 73, 165–179.
- Nichol, J.E., Bilal, M., 2016. Validation of MODIS 3 km resolution aerosol optical depth retrievals over Asia. *Remote Sens.* 8 (4), 328.
- Rajput, P., Sarin, M.M., Rengarajan, R., Singh, D., 2011. Atmospheric polycyclic aromatic hydrocarbons (PAHs) from post-harvest biomass burning emissions in the Indo-Gangetic Plain: isomer ratios and temporal trends. *Atmos. Environ.* 32 (45), 6732–6740.
- Ramana, M.V., Ramanathan, V., Feng, Y., Yoon, S.-C., Kim, S.-W., Carmichael, G.R., Schauer, J.J., 2010. Warming influenced by the ratio of black carbon to sulphate and the black-carbon source. *Nat. Geosci.* 3, 542–545.
- Ramanathan, Veerabhadran, Feng, Yan, 2009. Air pollution, greenhouse gases and climate change: global and regional perspectives. *Atmos. Environ.* 43 (1), 37–50.
- Ramanathan, V., Crutzen, P.J., Kiehl, J.T., Rosenfeld, D., 2001. Aerosols, climate, and the hydrological cycle. *Science* 294, 2119–2124.
- Reid, J.S., Eck, T.F., Christopher, S.A., Hobbs, P.V., Holben, B.N., 1999. Use of the Ångström exponent to estimate the variability of optical and physical properties of aging smoke particles in Brazil. *J. Geophys. Res.* 104 (D22), 27473–27489.
- Remer, L.A., Kleidman, R.G., Levy, R.C., Kaufman, Y.J., Tanré, D., Mattoo, S., Martins, J.V., Ichoku, C., Koren, I., Yu, H., Holben, B.N., 2008. Global aerosol climatology from the MODIS satellite sensors. *J. Geophys. Res. Atmos.* 113 (D14).
- Remer, L.A., Mattoo, S., Levy, R.C., Munchak, L.A., 2013. MODIS 3 km aerosol product: algorithm and global perspective. *Atmos. Meas. Tech.* 6, 1829–1844. <http://dx.doi.org/10.5194/amt-6-1829-2013>.

- Sayer, A.M., Hsu, N.C., Bettenhausen, C., Jeong, M.-J., 2013. Validation and uncertainty estimates for MODIS Collection 6 “Deep Blue” aerosol data. *J. Geophys. Res. Atmos.* 118, 7864–7872. <http://dx.doi.org/10.1002/jgrd.50600>.
- Sayer, A.M., Munchak, L.A., Hsu, N.C., Levy, R.C., Bettenhausen, C., Jeong, M.-J., 2014. MODIS Collection 6 aerosol products: comparison between Aqua's e-Deep Blue, Dark Target, and “merged” data sets, and usage recommendations. *J. Geophys. Res. Atmos.* 119, 13,965–13,989. <http://dx.doi.org/10.1002/2014JD022453>.
- Seinfeld, J.H., Bretherton, C., Carslaw, K.S., Coe, H., DeMott, P.J., Dunlea, E.J., Feingold, G., Ghan, S., Guenther, A.B., Kahn, R., Kraucunas, I., 2016. Improving our fundamental understanding of the role of aerosol – cloud interactions in the climate system. *Proc. Natl. Acad. Sci.* 113 (21), 5781–5790.
- Sen, A., Ahammed, Y.N., Banerjee, T., Chatterjee, A., Choudhuri, A.K., Das, T., Deb, N.C., Dhir, A., Goel, S., Khan, A.H., Mandal, T.K., 2016. Spatial variability in ambient atmospheric fine and coarse mode aerosols over Indo-Gangetic plains, India and adjoining oceans during the onset of summer monsoons, 2014. *Atmos. Pollut. Res.* 7 (3), 521–532.
- Sen, A., Abdelmaksoud, A.S., Ahammed, Y.N., Banerjee, T., Bhat, M.A., Chatterjee, A., Choudhuri, A.K., Das, T., Dhir, A., Dhyani, P.P., Gadi, R., 2017. Variations in particulate matter over Indo-Gangetic Plains and Indo-Himalayan Range during four field campaigns in winter monsoon and summer monsoon: role of pollution pathways. *Atmos. Environ.* 154, 200–224.
- Shi, Y., Zhang, J., Reid, J.S., Hyer, E.J., Hsu, N.C., 2013. Critical evaluation of the MODIS deep blue aerosol optical depth product for data assimilation over North Africa. *Atmos. Meas. Tech.* 6, 949–969. <http://dx.doi.org/10.5194/amt-6-949-2013>.
- Singh, N., Mhawish, A., Deboudt, K., Singh, R.S., Banerjee, T., 2017a. Organic aerosols over Indo-Gangetic Plain: sources, distributions and climatic implications. *Atmos. Environ.* 157, 59–74.
- Singh, N., Murari, V., Kumar, M., Barman, S.C., Banerjee, T., 2017b. Fine particulates over South Asia: review and meta-analysis of PM_{2.5} source apportionment through receptor model. *Environ. Pollut.* 223, 121–136.
- Smirnov, A., Holben, B.N., Eck, T.F., Dubovik, O., Slutsker, I., 2000. Cloud-screening and quality control algorithms for the AERONET database. *Remote Sens. Environ.* 73 (3), 337–349. [http://dx.doi.org/10.1016/S0034-4257\(00\)00109-7](http://dx.doi.org/10.1016/S0034-4257(00)00109-7).
- Sorek-Hamer, M., Cohen, A., Levy, R.C., Ziv, B., Broday, D.M., 2013a. Classification of dust days by satellite remotely sensed aerosol products. *Int. J. Remote Sens.* 34 (8), 2672–2688.
- Sorek-Hamer, M., Strawa, A.W., Chatfield, R.B., Esswein, R., Cohen, A., Broday, D.M., 2013b. Improved retrieval of PM_{2.5} from satellite data products using non-linear methods. *Environ. Pollut.* 182, 417–423.
- Sorek-Hamer, M., Kloog, I., Koutrakis, P., Strawa, A.W., Chatfield, R., Cohen, A., Ridgway, W.L., Broday, D.M., 2015. Assessment of PM_{2.5} concentrations over bright surfaces using MODIS satellite observations. *Remote Sens. Environ.* 163, 180–185.
- Tanré, D., Kaufman, Y.J., Herman, M., Mattoo, S., 1997. Remote sensing of aerosol properties over oceans using the MODIS/EOS spectral radiances. *J. Geophys. Res.* 102 (D14), 16,971–16,988. <http://dx.doi.org/10.1029/96JD03437>.
- Tripathi, S.N., Dey, S., Chandel, A., Srivastava, S., Singh, R.P., Holben, B.N., 2005. Comparison of MODIS and AERONET derived aerosol optical depth over the Ganga Basin, India. *Ann. Geophys.* 23, 1093–1101.
- Tripathi, S.N., Pattnaik, A., Dey, S., 2007. Aerosol indirect effect over Indo-Gangetic plain. *Atmos. Environ.* 41, 7037–7047.
- Van Donkelaar, A., Martin, R.V., Brauer, M., Kahn, R., Levy, R.C., Verduzco, C., Villeneuve, P.J., 2010. Global estimates of ambient fine particulate matter concentrations from satellite-based aerosol optical depth: development and application. *Environ. Health Perspect.* 118, 847–855.
- WHO, 2014. Burden of Disease. accessed on 10 February, 2017. World Health Organization. http://www.who.int/gho/phe/outdoor_air_pollution/urden_text/en/.